SYNTHESIS, SEPARATION, AND ISOLATION OF [6,6]-CLOSED EPOXIDE OF FULLERENE USING SEMI-PREPARATIVE HIGH PERFORMANCE LIQUID CHROMATOGRAPHY AND PREPARATION OF AQUEOUS COLLOIDAL SUSPENSIONS

A thesis presented to the faculty of the Graduate School of Western Carolina University in partial fulfillment of the requirements for the degree of Master of Science in Chemistry.

By

Jesse Raine Lazone Ingham

Director: Dr. Rangika Hikkaduwa Koralege

Assistant Professor of Chemistry

Department of Chemistry and Physics

Committee Members: Dr. Carmen Huffman, Chemistry

Dr. Channa De Silva, Chemistry

Dr. Nuwan Perera, Chemistry

April 2020

ACKNOWLEDGEMENTS

I would like to thank the various assistantships, whom have funded my living expenses throughout this research project: The WCU Summer 2019 Research Assistantship, WCU Department of Chemistry and Physics Alumni Scholarship, funding provided through my advisors Faculty Research and Creative Activities Award, and the many semesters of Teaching Assistantships.

I would like to give an extra special thank you to my research advisor, and mentor, Dr. Rangika Hikkaduwa Koralege, for her exceptional assistance and guidance throughout this entire project, and for making it a success. She has been a stalwart support for me throughout, and has become more than a teacher, advisor, and mentor and I will miss our daily debates and consults. I have learned so much from her and I trust we will remain in contact throughout my studies and career.

I would also like to thank my committee members, Dr. Carmen Huffman, Dr. Channa De Silva, and Dr. Nuwan Perera, for all of their guidance and assistance with this project. As well as Mr. Wes Bintz for all of the chemicals and supplies from the stockroom. I would like to thank Dr. Al Fischer for helping me to keep the instruments working, and in one piece. I would like to thank the following professors for their contributions to this project: Mr. Dan and Dr. Cynthia Atterholt, Dr.'s Charles and Deborah James, Dr. Brian Dinklemeyer, and Dr. Kathie Snyder. I would like to especially thank all of the professors of the graduate classes that I took.

I would also like to thank Mrs. Mitzy Garner, for her extensive work, long hours, and extra assistance on this project, and all of the past and present undergraduate students, whom

work in our lab: Keri Goff, Michael Gonzalez, and Christian Wyatt. As well as Makayla Yacuzzo, for her significant contributions over the summer.

I want to thank all of the undergraduate stockroom and prep-room students, whom prepared the teaching labs, and organized all of the chemicals, supplies, and waste throughout this project. A special thank you, to future Dr. Margaret Kocherga for her continued encouragement and support. I would also like to thank all of my friends who have helped me with this project, especially: Cecilia Baumgardner, Michael Bond, Susan Kenny, Katelyn Snyder, and Zay Watkins.

I would also like to thank all of the personally of the Facilities Management and Housekeeping Staff, whom helped to keep the building operational, and clean. I would like to especially mention: Kelly & Randy, Lisa, Sheila, Eddie, Tabitha, and Jay. As well as Mrs. Diann Ferguson and Carolyn Wiggins, for their continued assistance.

I would like to extend my deepest gratitude to my family, epically my mom, Debbie Stamper, and my brothers Bryen and Alik Hill for all of their help and support.

Lastly, I would like to thank the rest of the WCU Department of Chemistry and Physics, including all of the graduate and undergraduate researchers throughout the department.

TABLE OF CONTENTS

LIST OF TABLES

LIST OF FIGURES

LIST OF ABBREVIATIONS AND SYMBOLS

C_{60} – Buckminsterfullerene, fullerene
Nd:YAG – neodymium-doped yttrium aluminum garnet
℃ - degree Celsius
FCC – Frontier Carbon Corporation
Tol. – toluene
TCB – 1, 2, 4 – trichlorobenzene
n-Hex. – n-hexane
ACN. – acetonitrile
nC_{60} – nano-C_{60} – colloidal aggregates of C_{60}
SON – sonicator
THF – tetrahydrofuran
AQU – water
TTA – toluene, THF, and acetone
ROS – Reactive oxygen species
HDF – human dermal fibroblasts
HepG2 – human liver carcinoma cells
HPLC – high performance liquid chromatography
SP – semi-preparative
DLS – dynamic light scattering
O_2 – oxygen
N_2 – nitrogen
O_3 – ozone
ppm – parts per million
s – seconds
PSI – pounds per square inch
μg – microgram
μL – microliter
mL – milliliter
L/min – liter per minute
MP – mobile phase
SP – stationary phase
FR – flow rate
RT – retention time
RT – room temperature
UPW – ultrapure water
mW – milliwatt
nm – nanometer
λ – lambda
nm – nanometer
d.nm – diameter in nanometers
PDI – Polydispersity index

ABSTRACT

SYNTHESIS, SEPARATION, AND ISOLATION OF [6,6]-CLOSED EPOXIDE OF FULLERENE USING SEMI-PREPARATIVE HIGH PERFORMANCE LIQUID CHROMATOGRAPHY AND PREPARATION OF AQUEOUS COLLOIDAL SUSPENSIONS

Jesse R. L. Ingham

Western Carolina University, April 2020

Director: Dr. Rangika Hikkaduwa Koralege

Fullerenes are among the most attractive carbon nanomaterials and have wide-spread applications including electronics, automobile, aircraft, and energy. C_{60} has a tendency to form stable colloidal aggregates (also known as, nano-C_{60} or *n*C_{60}) in most aqueous conditions, making the *n*C_{60} form an important staring point and a fundamental model for comparing all fullerene impact studies. *n*C_{60} has been shown to induce toxicity in numerous cell cultures and whole animal systems. However, contradictory reports in the literature make it difficult to interpret the mechanism by which fullerene toxicity is induced. *n*C_{60} suspensions are demonstrated to rely on the [6,6]-closed epoxide ($C_{60}O$) derivative of the fullerene for stability. It is important to investigate the role of $C_{60}O$ in the observed oxidation behavior of fullerene aqueous suspensions. Our goal of this project is focused on the synthesis, separation, and isolation of $C_{60}O$ using semi-preparative high performance liquid chromatography, and preparation of colloidal suspensions. In the present study, we have successfully synthesized oxides of fullerene by ozonating solutions of C_{60} in toluene under ambient conditions. Excellent separation between C_{60}, $C_{60}O$, and $C_{60}O_2$ was achieved by using a mixture of toluene/n-hexane mobile phase in a Nacalai Cosmosil Buckyprep

semi-preparative column. Separated compounds were successfully isolated and analyzed by UV-Vis spectroscopy. The wavelengths of maximum absorbance were determined to be 336, 328, and 315 nm for C_{60}, $C_{60}O$, and $C_{60}O_2$, respectively and are in agreement with literature reported values. Ultimately, successful synthesis of aqueous suspensions of $C_{60}O$ was achieved, and the colloid composition was confirmed to be purely $C_{60}O$. Aqueous colloidal suspensions of $C_{60}O$ have an average hydrodynamic diameter of 140 ± 20 nm, with a PDI of 0.28 ± 0.05. To the best of our knowledge this is the first report of successful synthesis of colloidal suspensions of pure $C_{60}O$.

CHAPTER ONE: INTRODUCTION

1.1 – Background

Buckminsterfullerene (also known as, fullerene) was discovered by Richard E. Smalley and Robert F. Curl from Rice University and Sir Harold W. Kroto from the University of Sussex in 1985, all of whom were awarded the Nobel Prize of Chemistry in 1996.[1] The name fullerene was derived from R. Buckminster Fuller's geodesic architectural structures that resemble the proposed shape of the fullerene molecule.

The structure of C_{60} is made up of 20 hexagonal and 12 pentagonal surfaces, where each vertex is a carbon atom.[2] Figure 1 shows the 3 dimensional structure of C_{60}.[3] There are two distinct aromatic C=C bonds present in fullerene, the [6,6]- and the [5,6]- bonds, where [6,6]-bonds can be found at the edge between two hexagons and the [5,6]- bonds are between hexagons and pentagons.

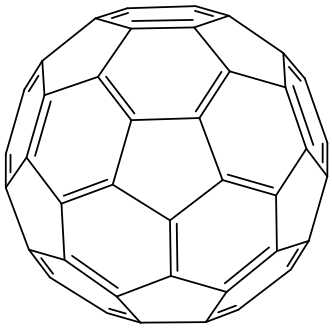

Figure 1: 3D Structure of C_{60}.

C_{60} is highly chemically and structurally stable; along with easily accepting protons, it can be easily purified and functionalized.[4] Kroto, *et al*. has successfully synthesized C_{60} by

vaporizing carbon from the surface of a disk of graphite into a high density helium flow with a focused Q-switched Nd:YAG laser. The carbon was then expanded in a supersonic molecular bean, photoionized, and detected by using time of flight – mass spectrometry.[5] Krätschmer, *et al*. described a different synthesis process involving evaporation of graphite electrodes in a 100 torr He atmosphere, which produced black soot. This soot was removed from collecting surfaces and dissolved in benzene or other organic solvents, and gently heated to concentrate the wine-red colored solution.[6] Alternatively, the soot can be sublimed, by heating to 400 ℃ in a vacuum (or inert atmosphere) to yield C_{60}.[6] C_{60} has been naturally found in shungite coal from the Kola Peninsula, in Russia.[7] In recent years the production of fullerenes was increased from 400 kg/year to 40 ton/year production, by Frontier Carbon Corporation (FCC), in Tokyo, Japan. FCC has plans to increase production to 1500 ton/year.[4] C_{60} has applications for use in products which include pharmaceuticals, fuel cells, circuits and electronics, gas storage, and reaction catalysts.[4]

As a result of continuing progress of nanotechnology and widespread research, relating to potential applications of fullerenes, the production, usage, and potential release of these materials to the environment has increased rapidly leading to concerns about increased human and environmental exposure. Despite the ultimate commercial significance of these materials, contradictory claims about their properties have led to significant interest among researchers on their biological and environmental impacts, raising C_{60} to a touchstone nanoparticle to study biological and environmental interactions.[8]

1.2 – Solubility of Fullerenes

The reported solubility of C_{60} is detailed in Table 1.[9,10]

Table 1: Reported fullerene solubility.

Solvent	Solubility (10^3 x Molarity)
Toluene	3.89
1,2,4 – Trichlorobenzene	11.8
n – Hexane	0.060
Water	1.8×10^{-21}

The low water solubility, however, does not reflect the larger issue of water availability of fullerenes. C_{60} has a tendency to form stable colloidal aggregates (also known as, nano-C_{60} or *n*C_{60}) in most aqueous conditions, making the *n*C_{60} form to be an important stating point and a fundamental model for comparing all fullerene impact studies.[11–14] Recent finding by Murdianti *et al*.[14] demonstrated that stability of aqueous fullerene colloidal suspensions relies on the [6,6]-closed epoxide derivative of the fullerene ($C_{60}O$). According to their report, conversion of only 4.2% of the fullerene molecules to the epoxide form would be sufficient to completely cover the surface of the particle, thereby presenting a hydrophilic interface to the surrounding water. Enriching C_{60} solids with the epoxide isomer of $C_{60}O$ have resulted in a significantly accelerated formation of the colloidal particles even under an inert atmosphere confirming that the epoxides present on the colloid surface are accountable for the stability of the colloids.[14] $C_{60}O$ can also be formed by solution phase ozonation of C_{60}, which generates ozonides to give either epoxide or oxidoannulene upon further dissociation via thermolysis, and photolysis, respectively as shown in Figure 2.[15] Uncontrolled ozonation conditions yields higher oxides such as $C_{60}O_n$ where n>1 as shown in Figure 3.

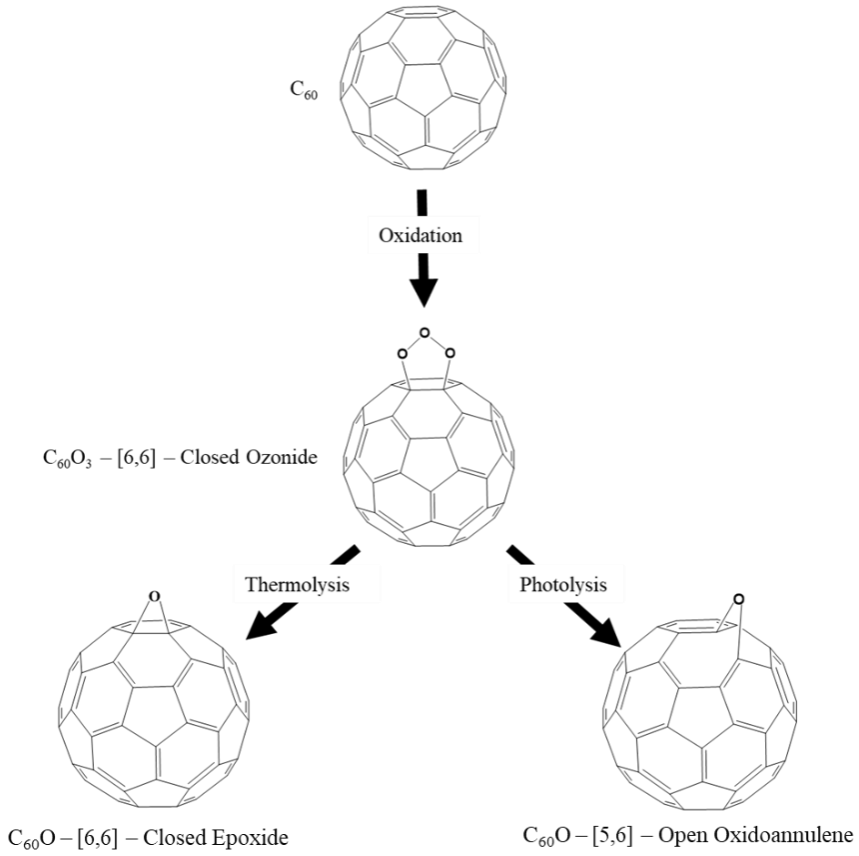

Figure 2: Reaction pathways for the formation of $C_{60}O$ isomers.

Covalent attachment of single functionalizing addend can yield up to four different isomeric products including, [6,6]-open, [6,6]-closed, [5,6]-open, and [5,6]-closed. Among these molecules, the [6,6]-closed and [5,6]-open isomers shown in Figure 2 are the most important isomers, where the functionalization happens at the junctions of two hexagons or across the single bonds at the hexagon-pentagon junction, respectively. Typically, the [5,6]-open derivatives are very unstable and they undergo conversion into the thermodynamically more stable [6,6]-closed isomers.[15]

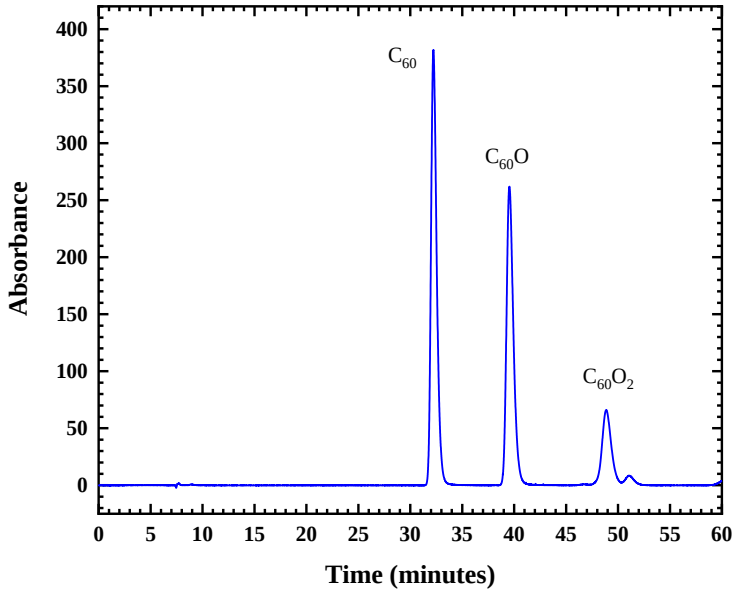

Figure 3: HPLC chromatogram showing the reaction of C_{60} with ozone producing higher oxides of fullerene.

There are several synthesis methods for synthesizing aqueous colloidal suspensions of C_{60} all of these methods will produce colloids of C_{60} with $C_{60}O$ on the surface. The amount of surface $C_{60}O$ coverage will depend on the ambient ozone levels. Maples, *et al.*[16] has described four synthesis techniques including, (1) the "SON" method, which utilizes a sonicator to evaporate the toluene from a solution of C_{60} in toluene, mixed with water, (2) the "THF" method, in which water is mixed with a C_{60} solution in THF and is removed by vigorous stirring, (3) the "AQU" method, where, C_{60} powder is left to stir, in water, for several months, open to the atmosphere, and (4) the "TTA" method, where a solution of C_{60} in toluene, is slowly transitioned to various solvents (toluene to THF to acetone to water), and the organic solvents are removed at each step.[16] In this research project, colloidal suspensions of pure $C_{60}O$ will be prepared as detailed in chapter 2 for future experimentation of their oxidative capacity.

1.3 – Oxidative Behavior of Fullerene

To date, significant amount of data have been reported in the literature providing conflicting interpretations of fullerene's health and environmental implications and cytotoxicity.[17,18] Studies that measured the results of oxidative damage reported it to be an oxidant,[14,19–21] while other studies which reported antioxidant activity or distinct lack of oxidation were in fact measuring the reactive oxygen species (ROS) proxies.[21] The first report on cytotoxicity of fullerene colloidal suspensions on human cell cultures was reported in 2004.[22] Sayes *et al*.[22] have observed oxidative damage to the cell membranes of human dermal fibroblasts (HDF) and human liver carcinoma cells (HepG2) *in-vitro*, were fullerene exposure led to cell death. Another study by Sayes,[20] in 2005, further confirmed that colloidal suspensions of C_{60} demonstrate significant toxicity in cell cultures including, lipid peroxidation. Another study by Oberdörster *et al*.[19] has highlighted that significant lipid peroxidation is observed in brains of largemouth bass after exposure to colloidal C_{60}. Some later findings attributed this oxidation to be entirely due to contaminants present in fullerene colloidal suspensions such as decomposition products of tetrahydrofuran , due to the synthesis procedures utilized.[20,21] Therefore, elucidating the extent and mechanism of oxidative toxicity caused by these materials will have profound implications for both designing environmentally friendly waste disposal methods for fullerenes and understanding fullerene/biological interactions in the environment.

1.4 – Research Goals and Expected Outcomes

This research project is focused on (1) synthesizing fullerene oxide ($C_{60}O$) enriched samples by ozonating C_{60} dissolved in toluene, (2) developing and optimizing a high-performance liquid chromatography (HPLC) method to separate $C_{60}O$, (3) developing and optimizing an isolation

method for $C_{60}O$ using semi-preparative HPLC, (4) synthesizing $C_{60}O$ aqueous colloidal suspensions, and (5) evaluating the colloidal properties, using DLS.

This work would develop optimal conditions/methods to synthesize $C_{60}O$ aqueous colloidal suspensions, which would enable the investigation of the oxidative behavior of these suspensions using probe-assisted spectroscopic determinations such as fluorescence spectroscopy and sophisticated kinetic data analysis techniques to elucidate mechanistic information. These findings will facilitate both designing environmentally friendly waste disposal methods for fullerenes, and understanding fullerene/biological interactions in the environment. Furthermore, the probe-assisted oxidation monitoring approach will provide useful insight into other mechanistic studies.

CHAPTER TWO: EXPERIMENTAL METHODS

2.1 – Materials

All the reagents were purchased from Sigma Aldrich or Fisher Scientific, unless otherwise indicated. The reagents were used without further purification. Ultrapure water (UPW) with a resistivity of 18.2 MΩ was obtained from a Barnstead EASYpure II RF/UV Ultrapure Water System.

2.2 – Preparation of C_{60} Stock Solutions and Dilutions

A stock solution of 2500 ppm (exact concentration 2450 ppm) C_{60} was prepared by dissolving 0.1225 g of pristine fullerene powder (Alfa Aesar 99.9% sublimed fullerene powder) in 50.0 mL of HPLC grade toluene (Alfa Aesar 99.7%). The resulting solution had a strong, deep, dark purple color, as shown in Figure 4. The sample was left to stir overnight.

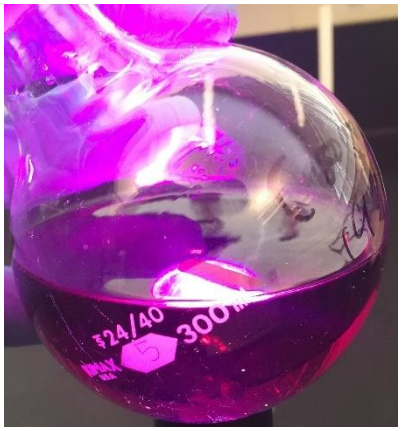

Figure 4: Illuminated C_{60} stock solution.

Diluted solutions were prepared by serial dilutions to achieve the specific concentrations. The diluted solutions were prepared to a final volume of 50.00 mL, for use in the ozonation

process. An example of a diluted sample is shown in Figure 5. The samples were left to stir overnight.

Figure 5: Diluted sample of C_{60}.

2.3 –Sample Ozonation Procedure

C_{60} solutions were ozonated using the apparatus shown in Figure 6. Ozone was produced by using a Longevity Resources Quantum 5 Ozone Generator. As shown in Figure 6, ozone was produced at the ozone generator, by using a stream of oxygen. The produced stream of ozone was mixed with a stream of nitrogen inside the glass gas manifold to produce a volume ratio of 1:4 of O_3:N_2 gases. This ozone/nitrogen mixture was purged through the system for 30 s to saturate the apparatus and tubing using a three-way Luer-lock valve. The gas mixture was bubbled into a three-neck round bottom flask containing a 406 ppm C_{60} solution dissolved in toluene, for a specific purge time as reported in Table 2. At the end of the purging period, the gas mixture was diverted to be vented into the fume hood as waste. During the entire ozonation process, the sample was magnetically stirred. After the ozonation was complete, the sample was stirred magnetically overnight.

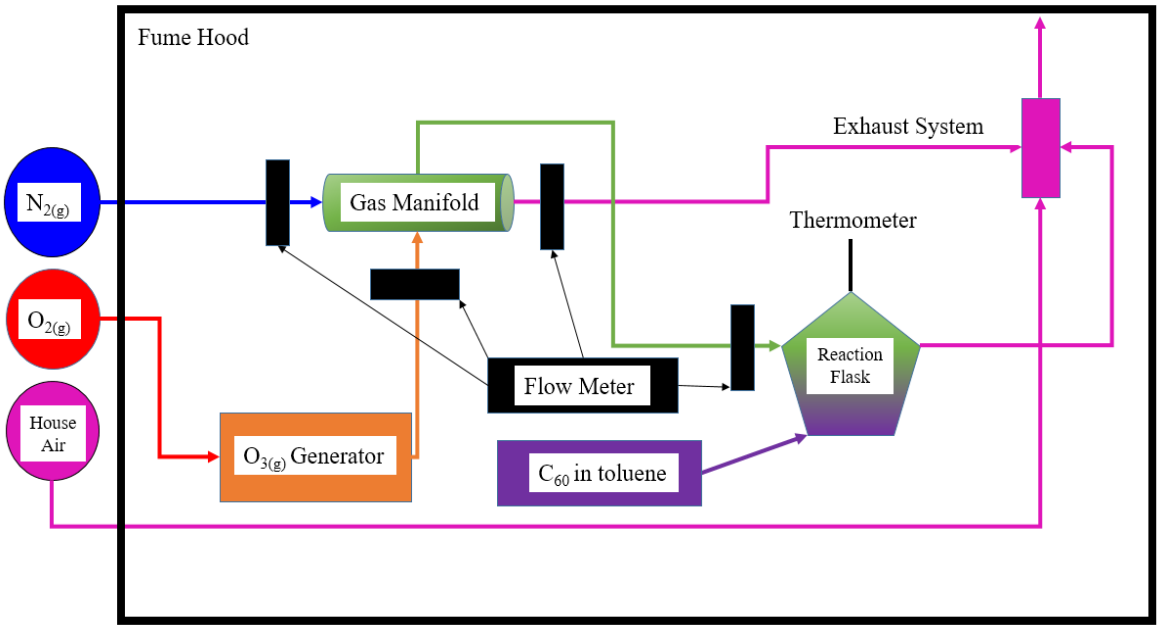

Figure 6: Schematic of ozonation apparatus.

The initial ozonation apparatus parameters for sample ozonation are described in Table 2. The ozone output was determined to be 4.7 μg/mL according to the output chart (Table 3) provided by the Longevity Resources Quantum 5 Ozone System Manual.

Table 2: Original ozonation parameters.

Ozonation Parameter	Selected Setting
Purge Time	30 s
Ozone Generator Concentration Output (Dial Setting)	2
Ozone Output Concentration	1.0 (μg/mL)
Oxygen Regulator Flow	1 L/min
Nitrogen Regulator Output Pressure	12 psi
House Air Flow	Minimal Flow
Nitrogen Flow Meter	0.8 L/min
Ozone Flow Meter	0.2 L/min
Nitrogen / Ozone Flow Meter	0.2 L/min
Waste Line Flow Meter	0.8 L/min
$C_{60\ (toluene)}$ Sample Concentration	403 ppm

Table 3: Ozone concentration output chart (μg/mL, adapted from Longevity Resources Quantum 5 Ozone System Manual).

O_2 Flow Rate		Ozone Concentration Output Setting on Generator									
L/min	cc/min	1	2	3	4	5	6	7	8	9	10
0.0625	62	10.3	18.8	27.0	34.7	47.1	59.9	78.5	93.8	108.7	123.4
0.125	125	5.1	9.6	14.1	18.5	26.0	34.1	47.6	60.3	74.1	90.5
0.25	250	2.6	5.1	7.6	10.1	14.3	19.2	27.2	35.6	45.5	58.3
0.5	500	1.3	2.6	4.0	5.3	7.6	10.3	15.0	19.8	25.6	33.7
0.75	750	0.6	1.4	2.3	3.1	4.5	6.2	9.0	12.1	15.9	21.1
1.0	1000	0.4	1.0	1.7	2.3	3.4	4.7	7.0	9.4	12.3	16.5
1.5	1500	0.2	0.7	1.1	1.6	2.4	3.3	5.0	6.7	8.9	12.0
2.0	2000	0.1	0.5	0.8	1.1	1.7	2.4	3.6	5.0	6.6	8.9

After the ozonation procedure, each sample was analyzed through a Thermo Dionex UltiMate 3000 HPLC with Multichannel Variable UV-Vis Detector. The column used was a Nacalai Cosmosil Buckyprep Packed Column (10.0 mm I.D. x 250 mm) equipped with a guard

column. The column was packed with high purity porous spherical silica gel particles, coated with 3-(1-pyrenyl) propyl stationary phase.

2.3.1 – Modifications in the Sample Ozonation Procedure

Using the original procedure outlined in Section 2.3, a variety of modifications were made to produce greater amounts of $C_{60}O$. The modifications are outlined in Table 4 and Table 5.

Table 4: Ozonation procedure modifications part 1.

Common Settings					
	N_2 Regulator (PSI):	12	N_2 Flow Meter (LPM):	0.8 LPM	
	Air Line Setting:	Minimal Setting	O_3 Flow Meter (LPM):	0.2 LPM	
	Waste Flow Meter (LPM):	0.8	N_2 / O_3 Mix Flow Meter (LPM):	0.2 LPM	
Adjusted Parameters					
Appendix Figure No.	Concentration (ppm)	Purge Time (s)	O_3 Generator Dial Setting	O_2 Regulator (LPM)	Ozone Output Concentration (µg/mL)
1	406	30	2	1	1.0
1	406	45	2	1	1.0
1	406	60	2	1	1.0
2	406	75	2	1	1.0
2	406	90	2	1	1.0
2, 4	404	120	2	1	1.0
3	404	90	4	1	2.3
3	404	90	6	1	4.7
3	404	90	8	1	9.4
3	404	90	10	1	16.5
4	404	120	6	1	4.7
4	404	120	8	1	9.4
4	404	120	10	1	16.5
5	403	150	6	1	4.7
5	403	180	6	1	4.7
5	403	210	6	1	4.7
6	616	120	6	1	4.7
6	821	120	6	1	4.7
6	1027	120	6	1	4.7
6	1324	120	6	1	4.7
6	1500	120	6	1	4.7
6	1764	120	6	1	4.7
6	1985	120	6	1	4.7
6	2206	120	6	1	4.7

Table 5: Ozone procedure modifications part 2.

	Common Settings						
	N_2 Regulator:	12 PSI	Purge Time (s):	120			
	Concentration (ppm):	403	Air Line Setting:	Minimal Setting			
Adjusted Parameters							
Appendix Figure No.	O_2 Regulator (LPM)	O_3 Flow Meter (LPM)	N_2 Flow Meter (LPM)	N_2 / O_3 Mix Flow Meter (LPM)	Waste Flow Meter (LPM)	O_3 Generator Dial Setting	Ozone Output Concentration (µg/mL)
Adjusted Parameters No. 1							
7	1.5	0.7	0.8	0.2	0.8	7	5.0
Adjusted Parameters No. 2							
7	1.5	0.7	0.8	0.2	0.3	7	5.0
Adjusted Parameters No. 3							
7	1	0.2	0.8	0.5	0.5	6	4.7

2.3.2 – Optimized Ozonation Procedure

In order to produce the maximum concentration of $C_{60}O$, with a minimum amount of higher oxides being produced, various ozonation parameters were adjusted, including the purge time, concentration, generator setting, and gas regulator pressures and outputs. After analyzing these adjustments, the optimal ozonation parameters were determined. Briefly, the parameters used a 2000-2500 ppm sample, a purge time of 120 seconds, and an ozone output of 4.7 µg/mL; a detailed listing of the parameters are reported in Table 6.

Table 6: Optimized ozonation parameters.

Ozonation Parameters	Selected Setting
Purge Time	120 s
Ozone Generator Concentration Output (Dial Setting)	6
Ozone Output Concentration	4.7 (μg/mL)
Oxygen Regulator Flow	1 L/min
Nitrogen Regulator Output Pressure	12 psi
House Air Flow	Minimal Flow
Nitrogen Flow Meter	0.8 L/min
Ozone Flow Meter	0.2 L/min
Nitrogen / Ozone Flow Meter	0.2 L/min
Waste Line Flow Meter	0.8 L/min
$C_{60\ (toluene)}$ Sample Concentration	2000 ppm

2.4 – Ozonation Under Different Conditions

2.4.1 – Ozonation Under Ambient Light

The original ozonation procedure for C_{60} dissolved in toluene was reported by Murdianti, et al.[14] We have used a slightly modified procedure of the original procedure reported and optimized ozonation parameters as discussed in section 2.3.2. The entire ozonation process was done under ambient light. An example of the sample color observed before and after ozonation is depicted below, in Figure 7.

Figure 7: Sample color before (left) and after ozonation (right).

2.4.2 – Ozonation Under Dark

Samples were ozonated using the same parameters outlined in Section 2.3.2, with the exception that the ozonation process was performed entirely in the dark. This experiment was completed at night, with the lab windows covered in either blinds or foil, and the overhead lights turned off. The mixing flask was wrapped top to bottom with aluminum foil during the ozonation to keep any stray light out of the flask. The only lights in use, was the use of red headlamps, so that the experiment could be performed. After the ozonation was complete, the sample was stirred magnetically overnight.

2.4.3 – Ozonation Under Fluorescent Light

Samples were ozonated using the same parameters outlined in Section 2.3.2, with the exception that the ozonation process was performed entirely under fluorescent light. Throughout the ozonation process, two, four-foot-long bar styled Jumpstart Hydro Farm fluorescent plant grow lights were used to provide fluorescent light directly on the sample. These fluorescent grow lights were used in conjunction with the fluorescent overhead laboratory lights, and fume hood lights. Throughout the ozonation process, and the overnight stirring, the grow lights were lowered to as close as possible to the stirring sample flask. After the ozonation process was

complete, the sample was left to stir overnight. The resulting color change went from a dark purple to a dark red, as shown in Figure 8.

Figure 8: Enriched C_{60} Sample.

2.5 – HPLC Analysis of Ozonated Fullerene Samples

Ozonated samples were analyzed using a Thermo Dionex UltiMate 3000 HPLC with Multichannel Variable UV-Vis Detector. The column used was a Nacalai Cosmosil Buckyprep Packed Column (10.0 mm I.D. x 250 mm) equipped with guard column. The stationary phase of the column consisted of high purity porous 5 μm spherical silica with a pyrenylpropyl functional group.

2.5.1 – Optimization of High Performance Liquid Chromatography Mobile Phases

A variety of mobile phases and gradients were tested in order to achieve excellent separation between C_{60}, $C_{60}O$, and $C_{60}O_2$ sample peaks and are summarized in Table 7.

Table 7: Summarized modified HPLC separation parameters.

Appendix Figure No.	Injection Volume (μL)	Flow Rate (mL / min)	Run Time (min)	Mobile Phase			
8, 9, 10	100	2.000	60.00	Toluene	100%		
8	100	2.000	60.00	Toluene	90%	Acetonitrile	10%
8	100	2.000	90.00	Toluene	70%	Acetonitrile	30%
8	100	5.000	60.00	Toluene	70%	Acetonitrile	30%
9	100	2.000	60.00	Gradient No. 1			
			(1-25)	Toluene	85%	n-Hexane	15%
			(25-45)	Toluene	75%	n-Hexane	25%
			(45-60)	Toluene	85%	n-Hexane	15%
9	100	2.000	60.00	Gradient No. 2			
			(1-22)	Toluene	85%	n-Hexane	15%
			(22-40)	Toluene	70%	n-Hexane	30%
			(40-60)	Toluene	85%	n-Hexane	15%
10	100	2.000	60.00	Toluene	95%	n-Hexane	5%
10	100	2.000	60.00	Toluene	85%	n-Hexane	15%
10	100	2.000	60.00	Toluene	80%	n-Hexane	20%
10	100	2.000	60.00	Toluene	75%	n-Hexane	25%
NI*	50	2.000	60.00	Toluene	70%	n-Hexane	30%
NI*	100	2.000	60.00	Toluene	70%	n-Hexane	30%
NI*	200	2.000	60.00	Toluene	70%	n-Hexane	30%
10	100	2.000	60.00	Toluene	70%	n-Hexane	30%

*Not included.

The optimized HPLC parameters for semi-preparative analysis are outlined in Table 8. Detector wavelengths for different compounds of fullerene and toluene are given in Table 9.

Table 8: Optimized parameters for HPLC separations.

Injection Volume (μL)	Mode	Flow Rate (mL / min)	Run Time (min)	Mobile Phase	
2500	Semi-Prep	2.000	60.00	Toluene	70%
				n-Hexane	30%

Table 9: Detector wavelengths for different compounds.

Channel Number	Detector Wavelength (nm)	Respective Compound
1	336	C_{60} (Tol.)
2	328	$C_{60}O$ (Tol.)
4	285	Toluene Solvent

For sample separation, the samples were collected in one-minute intervals, starting from retention times of 36 to 42 minutes. Figure 9 shows an example chromatogram with the fraction times marked. These seven, 2 mL, fractions were then re-analyzed to determine the composition.

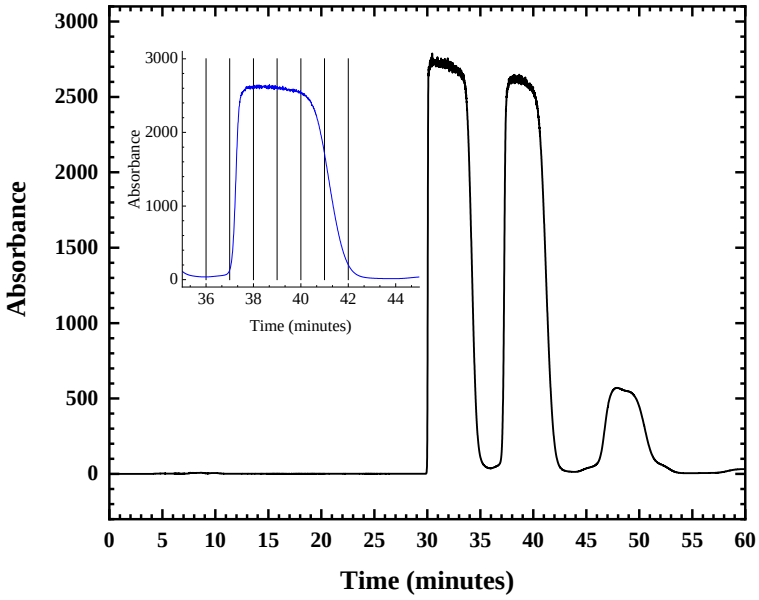

Figure 9: Example semi-preparative HPLC chromatogram with extraction time intervals shown in the inset.

2.5.2. – Isolation of Separated Compounds from HPLC

C_{60}, $C_{60}O$, and $C_{60}O_2$ compounds were isolated from HPLC, by using a five-port multichannel valve (Figure 11). The multichannel valve was positioned just beyond the detector casing of the HPLC (Figure 10). In normal operation, the valve would direct the instrument outflow towards

the waste container, whereas in isolation operation, the valve would be directed to a 20 mL vial. For isolating $C_{60}O$, the multi-port valve was opened at a retention time (RT) of 36 minutes, and one-minute fractions were collected between a RT of 36 and 42 minutes. A chromatogram with the peak partitions is depicted in Figure 9, which shows the one-minute fractions isolated from HPLC. The same procedure was used to isolate pure samples of C_{60} and $C_{60}O_2$ at their retention times.

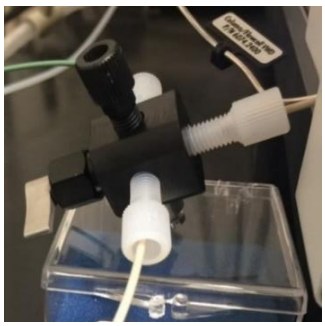

Figure 10: Multiport valve.

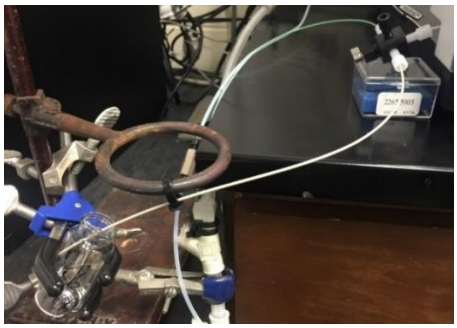

Figure 11: Isolation apparatus, with vial, during sample collection.

2.5.3 – HPLC Re-analysis of Isolated Fractions

The isolated fractions were re-analyzed, to determine the purity of the fractions for each compound. As reported in the Section 3.5, samples that contained a concentration ratio of $C_{60}O$:C_{60} greater than 100 were used to prepare aqueous suspensions of $C_{60}O$ for further analysis. The instrument parameters used for the re-analysis is outlined in Table 10.

Table 10: Optimized re-analysis parameters for HPLC sample fractions.

Injection Volume (µL)	Mode	Flow Rate (mL / min)	Run Time (min)	Mobile Phase	
100	Analytical	2.000	60.00	Toluene	70%
				n-Hexane	30%

2.6 – Preparation of $C_{60}O$ Aqueous Colloidal Suspensions

2.6.1 – Method Optimization for Solvent Exchange from Toluene to Water to Produce Aqueous Suspensions of $C_{60}O$

As reported in Section 3.5, samples that contained a concentration ratio of $C_{60}O$:C_{60} greater than 100 were combined for the solvent exchange process. These samples will be referred to as "$C_{60}O$ enriched" samples.

2.6.2 – Stirring Method

The extracted $C_{60}O$ enriched sample, was added to a round bottom flask and rotary evaporated until completely dry, as outlined in Table 11. This procedure was repeated with several $C_{60}O$ enriched samples until dry and the flasks were left open inside a fume hood for a few days to remove any toluene residues left after rotary evaporation. 10 mL of ultrapure water (UPW) was added to the resulting dried solid $C_{60}O$ samples. This mixture was stirred for a month to achieve aqueous suspension of $C_{60}O$.

Table 11: Example rotary evaporation parameters.

Rotary Evaporator Speed (RPM)	Water Bath Temperature (℃)	Vacuum Pressure (mmHg)	Amount of UPW Added (mL)
220	80	-508	2

2.6.3 – Rotary Evaporation Method with Ultrapure Water

The extracted $C_{60}O$ enriched samples were rotary evaporated with small amounts of ultrapure water to slowly evaporate off the toluene, in order to produce an aqueous sample. Rotary evaporation parameters used are listed in Table 11.

2.6.4 – Rotary Evaporation Combined with Sonicator and Shaker

The extracted, $C_{60}O$ enriched samples were condensed using rotary evaporation, and then a small amount of ultrapure water were added to the condensed $C_{60}O$ samples. Where two layers were formed, the top most being the condensed $C_{60}O$ sample dissolved in toluene, and the bottom being UPW. The sample was then sonicated for several hours to evaporate any leftover toluene, and then shaken on a Thermo Scientific MaxQ 2000 shaker for several days to yield aqueous suspensions of $C_{60}O$.

2.6.5 – Centrivap Method

The extracted $C_{60}O$ enriched samples were partitioned equally between four 1.5 mL vials, were it was mixed with 0.75 mL ultrapure water. Several water blanks were used to counterbalance the mass. Using the settings below (Table 12), the centrifuge was run under a specified pressure, until the organic solvent had evaporated.

Table 12: Centrivap experimental parameters.

Temperature (℃)	Rotation Speed	Vacuum Pressure (mmHg)
RT	"On"	-635
35	"On"	-508
RT	"On"	-508

2.6.6 – Rotary Evaporation Combined with Sonicator

The extracted $C_{60}O$ enriched sample fractions were mixed with various volumes of ultrapure water, and were rotary evaporated using a customized rotary evaporator assembly. The customized assembly was composed of a Buchi condensing coil, a Heindorff rotovap motor and stand, and a VWR B1500A-MT sonicator bath. An example set of parameters used were

detailed in Table 13. Each sample was run until the organic solvent had evaporated, leaving the aqueous sample behind.

Table 13: Rotary evaporator-sonicator parameters.

Rotary Evaporator Speed (RPM)	Sonicator Status	Sonicator Temperature (℃)	Vacuum Pressure (mmHg)	Amount of UPW Added (μL)
280	On	RT	-457	6000

2.6.7 – Optimized Solvent Exchange Method

Extracted fractions were mixed with 6000 μL of ultrapure water, and immediately rotary evaporated using a customized rotary evaporator assembly. The customized rotary evaporator assembly was composed of a Buchi condensing coil, a Heindorff Rotovap Motor and stand, and a VWR B1500A-MT Sonicator Bath. The parameters used were outlined in Table 14. Each sample was run until the organic solvent had evaporated. Typically, the layered pink and clear separated layers will turn in to a pale-yellow color after the organic solvent has evaporated. Samples were then refrigerated for preservation.

Table 14: Optimized rotary evaporator-sonicator parameters.

Rotary Evaporator Speed (RPM)	Sonicator Status	Sonicator Temperature (℃)	Vacuum Pressure (mmHg)	Amount of UPW Added (μL)	Approximate Sample Run Time (min)
280	On	RT	-457	6000	7 – 8

2.7 – HPLC Re-analysis of Prepared Aqueous Colloids

$C_{60}O$ aqueous colloidal samples were subjected to a solvent exchange from water to toluene in order to confirm the composition of the colloids by HPLC.

Two mL of a 10% (W/V) $NaNO_3$ and 2 mL of HPLC grade toluene was added to a 20-mL vial. 1 mL of the $C_{60}O$ aqueous colloidal sample was filtered with a wet 0.45-micron syringe filter, and added to the vial. The mixture was stirred overnight and then the toluene and water layers were allowed to separate. The toluene layer was extracted and dried using anhydrous Na_2SO_4, and filtered through a 0.02 μm Whatman® Anatop™ filter before analyzing on the HPLC. These samples were re-analyzed using the same parameters outlined in Section 2.5.3, in Table 10.

2.8 – Characterization of $C_{60}O$ Aqueous Colloidal Suspensions

Aqueous $C_{60}O$ samples were analyzed to determine the maximum absorption wavelengths, particle size, and surface charge.

2.8.1 – UV-Vis Characterization

Using a 1.5 mL quartz cuvette (Figure 12), the C_{60}, $C_{60}O$, and $C_{60}O_2$ samples were analyzed using an Agilent Cary 5000 UV-Vis-NIR Spectrometer. The sample was scanned in double beam mode, with a toluene solvent blank, and a zero/baseline correction, from 800-200 nm.

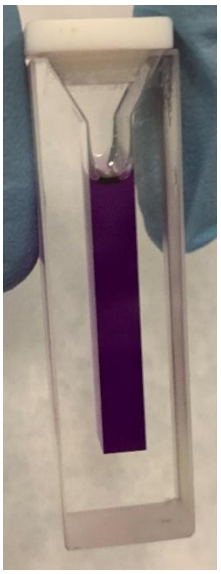

Figure 12: 1.5 mL UV-Vis quartz cuvette containing C_{60} sample.

2.8.2 – Determination of Colloidal Particle Size using DLS

The size distribution of the aqueous $C_{60}O$ colloidal particles was determined using DLS on a Malvern Zetasizer ZS Particle Size Analyzer equipped with a 4 mW 632.8 nm laser. All the measurements were done at 25 °C and using a Brand Tech Scientific ZEN0040 70 μL Ultra-Micro disposable cuvette, with stopper.

CHAPTER THREE: RESULTS AND DISCUSSION

3.1 – Optimization of Ozonation Parameters

As the solutions of C_{60} dissolved in toluene are ozonated, the C_{60} undergoes an oxidation reaction to produce different oxides of fullerene as shown below.[15,23] The goal of this optimization procedure was to acquire the best set of parameters to synthesize highest amount of $C_{60}O$. By optimizing the ozonation procedure, our goal is to maximize the amount of $C_{60}O$ while minimizing the formation of higher oxides. Parameters such as, starting concentration of C_{60}, ozone purging time and ozone concentration are contributing factors for the amount of oxides formed in the reaction.

$$C_{60} + O_3 \rightarrow C_{60}O + C_{60}O_2 + \text{higher oxides} \qquad [1]$$

A typical HPLC chromatogram before optimization as discussed in procedure Section 2.3 is shown in Figure 13, and the sample retention times are reported in Table 15. As shown in the chromatogram, C_{60} eluted first, followed by $C_{60}O$ and $C_{60}O_2$. Fullerene compounds, C_{60}, $C_{60}O$, and $C_{60}O_2$ have higher affinity toward the 3-(1-pyrenyl) propyl stationary phase due to π interactions between the fullerene cage and the pyrenyl group. Non-polar nature of the mobile phase facilitates partitioning of non-polar analytes from the compounds mentioned above, and therefore C_{60} will elute first. As the polarity of the compounds increases by having more oxygens attached to the fullerene cage, retention time would increase.

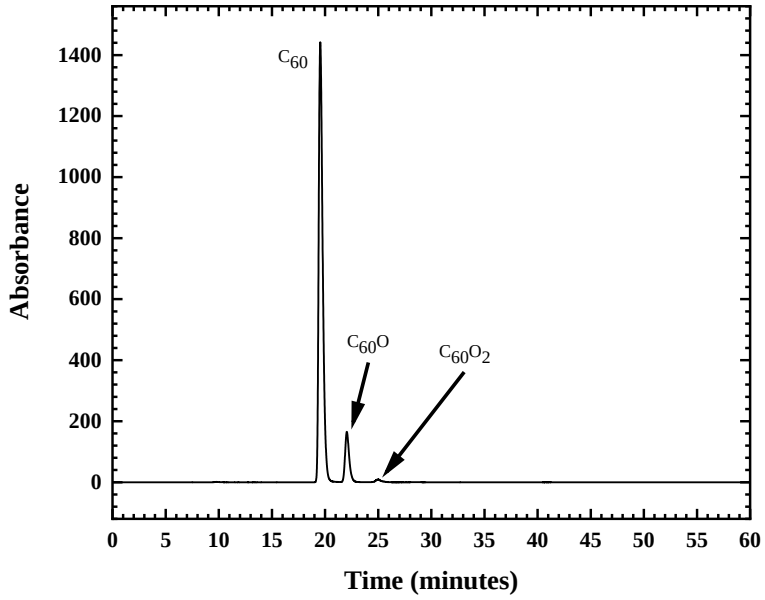

Figure 13: HPLC chromatogram of C_{60} and oxides.

Table 15: Sample retention times.

Component	Solvents	C_{60}	$C_{60}O$	$C_{60}O_2$
Time (min)	9.7	19.5	22.0	25.0

In order to achieve maximum amount of $C_{60}O$, the ozonation parameters were modified as listed in procedure Section 2.3.1. Several example chromatograms after the modifications are shown in Figure 14. All other chromatograms are included in Appendix A.

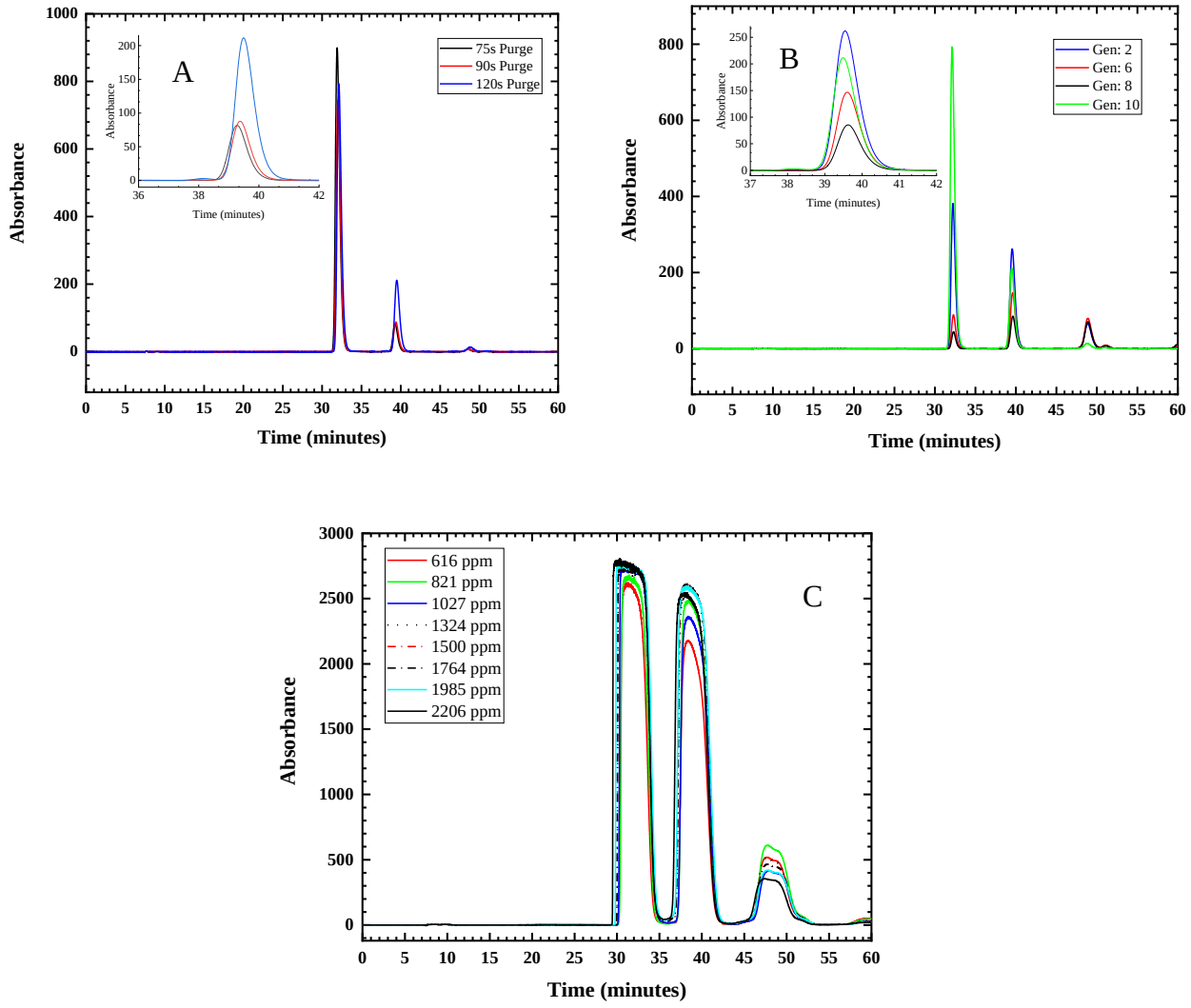

Figure 14: Ozonation optimization chromatograms. (A) Different purge times, (B) Different ozone generator settings, and (C) Different starting C_{60} concentrations.

As the purge time is increased, more $C_{60}O$ is produced, however, by using a longer purge times, higher amounts of higher oxides were produced as shown in Figure 14 A. As the dial setting on the ozone generator was increased, higher concentrations of ozone were produced. As the concentration of O_3 increased at a purge time of 120 s, the amount of oxides produced increased. But the amount of C_{60} remained in solution was high compared to the oxides formed

as evidenced by Figure 14 B. As the initial C_{60} sample concentration was increased, the concentration of $C_{60}O$ also increased, until the HPLC detector became saturated, as seen by the flattened apex of the semi-preparative chromatograms shown in Figure 14 C. After analyzing these adjustments, the optimal ozonation parameters were determined. Briefly, the parameters used a 2000-2500 ppm sample, a purge time of 120 seconds, and an ozone output of 4.7 μg/mL; a detailed listing of the parameters are reported in Chapter 2, Table 6.

A semi-preparative chromatogram resulted from optimized ozonation procedure is shown in Figure 15. Although the peaks were baseline resolved, peak separation retention times were not adequate for isolating each compound from the column. Therefore, optimization of mobile phase conditions was important to achieve maximum retention time separation between the compounds.

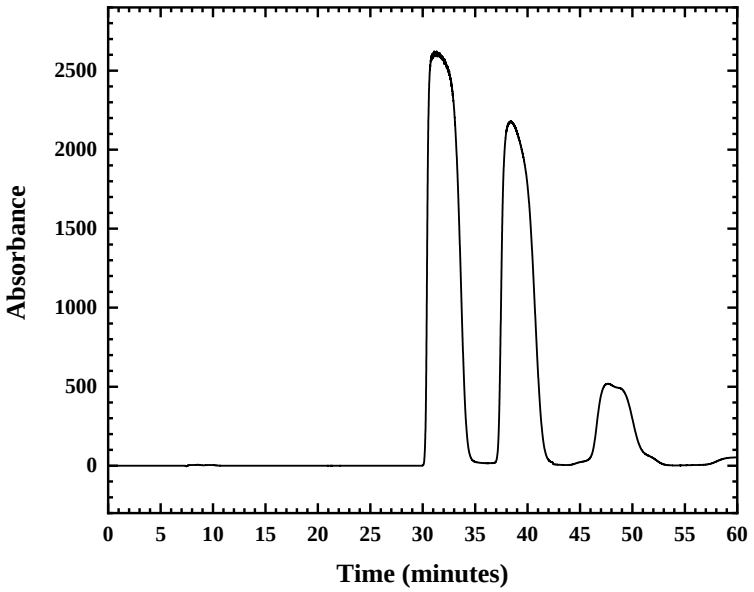

Figure 15: Semi-preparative chromatogram resulted from optimized ozonation procedure.

3.2 – Optimization of High Performance Liquid Chromatography Mobile Phases

A variety of mobile phases and gradients were tested in order to achieve excellent separation between C_{60}, $C_{60}O$, and $C_{60}O_2$ sample peaks and are summarized in Table 7 of Chapter 2. For example, by using a 100% toluene mobile phase (MP), and a flow rate of 2.000 mL/min, the retention times for C_{60}, $C_{60}O$, and $C_{60}O_2$ were 19.6, 22.1, and 25.0 minutes, respectively. By using a mixture of toluene/acetonitrile (ACN) (70:30), and a flow rate of 2.000 mL/min, the resulting retention times for C_{60}, $C_{60}O$, and $C_{60}O_2$ were 60.1, 65.5, and 71.0 minutes, respectively. Two gradient mixtures were tested as well, by using the gradient parameters No. 2 shown in Table 6, and a flow rate of 2.000 mL/min. The resulting retention times for C_{60}, $C_{60}O$, and $C_{60}O_2$ were 23.9, 28.0, and 34.8 minutes, respectively. These mobile phases were able to provide a good baseline separation for compounds, but the separations were not enough to isolate each compound individually. By using a mixture of toluene/n-hexane (70:30), and a flow rate of 2.000 mL/min, we were able to achieve the maximum separation between compounds, C_{60}, $C_{60}O$, and $C_{60}O_2$ and the retention times are reported as 32.1, 39.4, and 48.7 minutes, respectively. Several example chromatograms are shown in Figure 16, with an example of a semi-preparative chromatogram shown in Figure 16 E below and all other chromatograms are included in Appendix A for further reference.

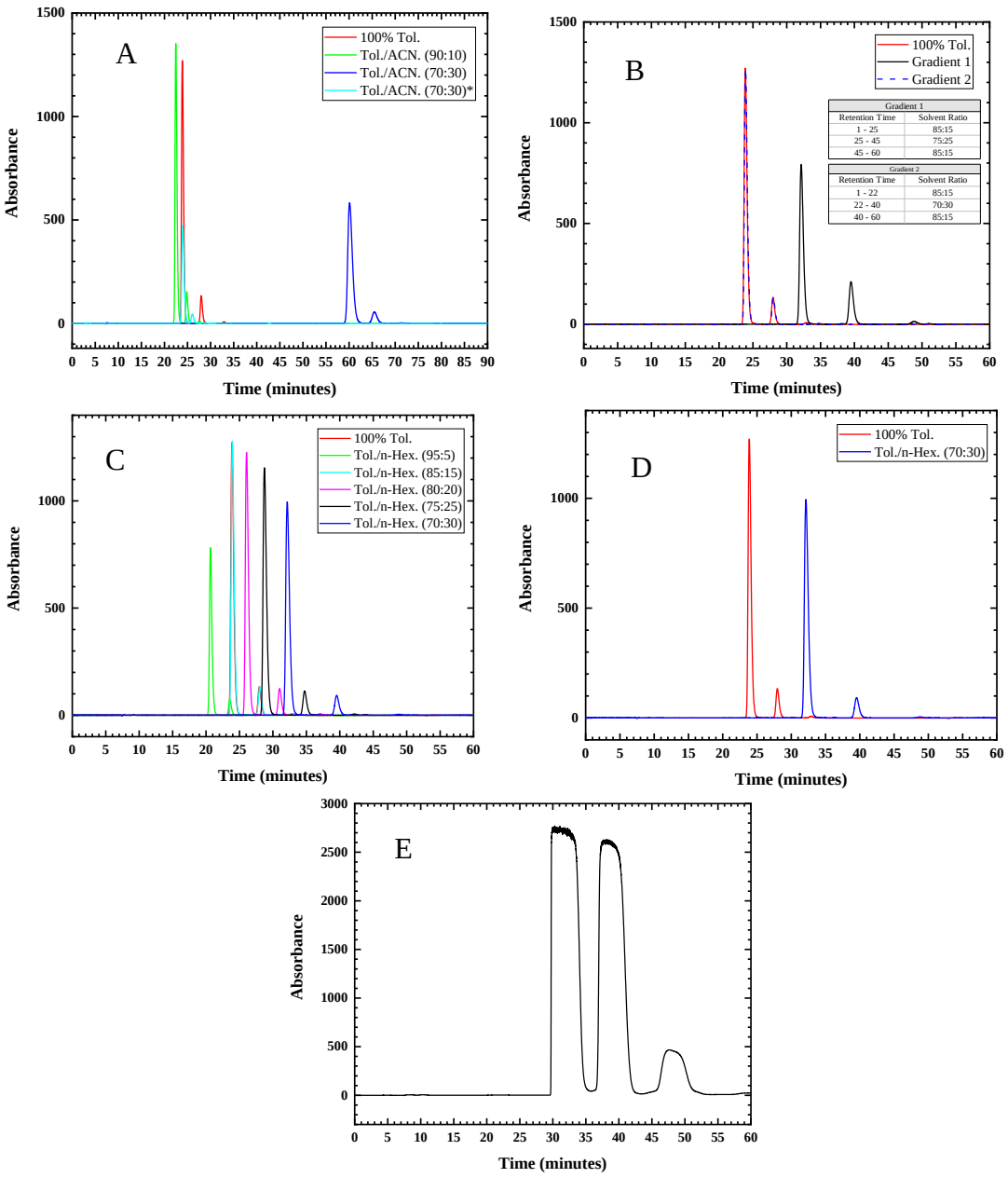

Figure 16: Example chromatograms from the HPLC optimization. (A) 100 µL Injection of a 406 ppm sample, using various mobile phase mixtures of toluene and acetonitrile (ACN.) using a flow rate of 2.000 mL/min. *Used a flow rate of 5.000 mL/min, (B) 100 µL Injection of a 406 ppm sample, using various gradient mobile phase mixtures of toluene and n-hexane (i.e. 85:15), using a flow rate of 2.000 mL/min, (C) 100 µL Injection of a 406 ppm sample, using a mobile phase of toluene and n-hexane (70:30), and a flow rate of 2.000 mL/min, (D) 100 µL Injection of a 406 ppm sample, using a mobile phase of toluene and n-Hexane (70:30), and a flow rate of 2.000 mL/min, and (E) 2500 µL injection, toluene/n-hexane (70:30).

3.3 HPLC Analysis of Ozonated Fullerene Oxides

The ozonated fullerene samples were analyzed through analytical mode HPLC using low sample volumes of 100 μL, to determine the elution order and retention times of the compounds. Figure 17 demonstrates a typical analytical mode HPLC chromatogram of fullerene oxides with an excellent baseline peak separation.

Table 16 indicates the retention times and λ_{max} values of fullerene and two different oxides. Identity and the order of elution of these oxides were confirmed by retention times and by comparing reported λ_{max} values of each oxide with measured λ_{max} for each compound using UV/vis spectroscopy (Figure 18).[14,15,24]

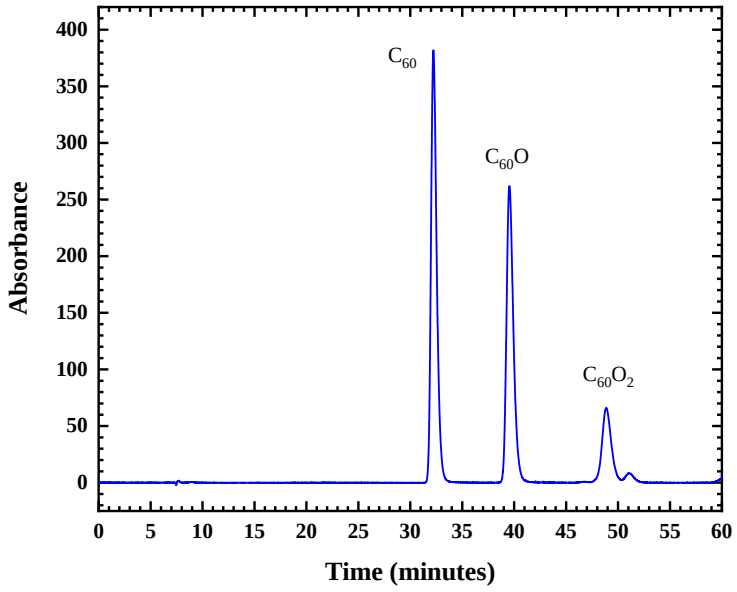

Figure 17: Example of analytical mode chromatogram, with baseline peak separation.

Table 16: Retention times and λ_{max} values for fullerene and the first two oxides.

Compound	λ_{max} reported (nm)	λ_{max} experimental (nm)	Retention Time (min)
C_{60}	336[a]	336	32
$C_{60}O$	328[b]	328	40
$C_{60}O_2$	314[c]	315	49

a *Murdianti, et al.*[14]
b *Murdianti, et al.*[14]
c *Heymann*[25]

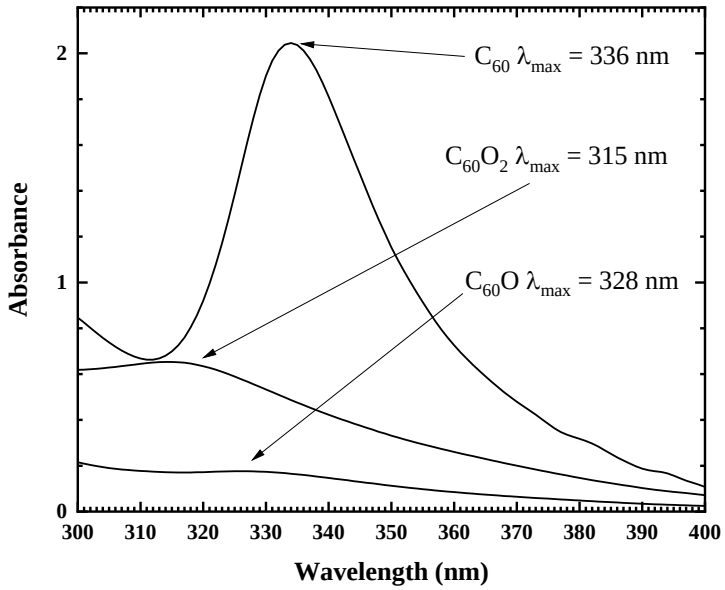

Figure 18: UV-Vis spectra showing the λ_{max} values for C_{60}, $C_{60}O$, and $C_{60}O_2$.

As discussed in Section 3.1, C_{60}, $C_{60}O$, and $C_{60}O_2$ have higher affinity toward the 3-(1-pyrenyl) propyl stationary phase due to π interactions between the fullerene cage and the pyrenyl group. However, the non-polar nature of the mobile phase facilitates partitioning of non-polar analytes. As the polarity of the compounds increases by having more oxygens attached to the fullerene cage, retention time would increase. C_{60} is the least polar of the compounds shown above and it will elute first, followed by $C_{60}O$ and $C_{60}O_2$, respectively.

The UV-Vis absorption bands of C_{60} in toluene correspond to the electronic transitions of $\pi \rightarrow \pi^*$ and $n \rightarrow \pi^*$. Experimental and literature reported λ_{max} values of C_{60}, $C_{60}O$, and $C_{60}O_2$ resulted from intense $\pi \rightarrow \pi^*$ transition band in the ultraviolet region are reported in

Table 16.[26,27] There is a shift of absorption maximum to a shorter wavelength from 336 to 315 nm due to substitution, known as hypochromic effect or a blue shift seen in these compounds. As an increasing number of oxygens are added to the fullerene cage, the π-system electrons are disrupted, which causes the shift in the local absorption maxima, towards the blue.[25,28]

3.4 – Semi-Preparative HPLC Separation and Isolation of Fullerene Epoxide

In order to isolate $C_{60}O$ from C_{60} and the other oxides, a semi-preparative HPLC equipped with a large sample loop with an injection volume of 2500 μL was used. By using a highly-concentrated sample of ozonated C_{60} with a concentration of 2000 ppm, and other parameters detailed in Section 2.3.2, excellent baseline peak separation between the compounds was achieved. The retention time of each compound was adequate for clearly isolating each compound. Figure 19 shows a semi-preparative HPLC chromatogram with the order of elution for each compound. As seen in the chromatogram, the high concentration of the samples has resulted in peak broadening, which is caused by longitudinal and Eddy diffusion.[29] Longitudinal and Eddy diffusions are caused by the increase in time and the difference in flow streams, within the column, respectively.[29] The flat apex of the peaks, is caused by detector saturation.[29]

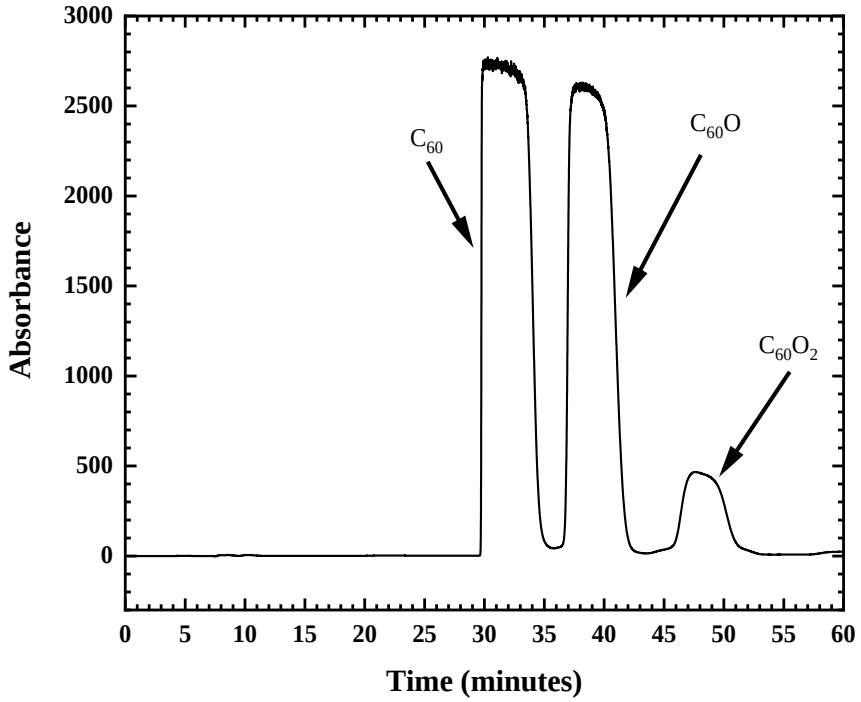

Figure 19: Semi-preparative chromatogram showing peaks for C_{60}, $C_{60}O$, and $C_{60}O_2$.

Figure 20 depicts a lineup of fullerene and two different fullerene oxides isolated through HPLC. C_{60}, $C_{60}O$, and $C_{60}O_2$ fractions showing colors of dark purple, reddish pink, and faint pinkish yellow, respectively. As the fractions are eluted, the samples become more diluted, which contributes to the decreasing intensity of the sample color.

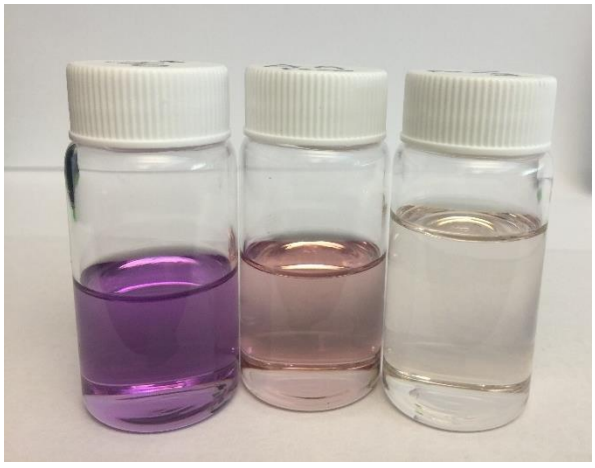

Figure 20: Extracted samples of C_{60}, $C_{60}O$, and $C_{60}O_2$, respectively.

3.5 – HPLC Re-analysis of Isolated Fractions

Separated samples were individually isolated as fractions, using the procedure outlined in Section 2.5.3. For $C_{60}O$, the extraction times were determined to be between 36 and 42 minutes, as the retention time spans over seven minutes. These samples were re-analyzed through HPLC to confirm the purity of each compound. As reported in Table 17, samples that contained a concentration ratio of $C_{60}O$:C_{60} greater than 100 were used to prepare aqueous suspensions of $C_{60}O$ for further analysis. Figure 21 shows a typical semi-preparative HPLC chromatogram, with the $C_{60}O$ fractions isolated has included as an inset graph. Figure 22 depicts these seven fractions, and their observed colors ranging from colorless to pink back to colorless, across the sample lineup.

Table 17: Calculated concentration ratios of $C_{60}O$:C_{60} in the re-analysis fractions.

Fraction # (minutes)	$C_{60}O$ peak height (AU) at 328 nm	C_{60} peak height (AU) at 336 nm	Concentration Ratio $C_{60}O$:C_{60}
36	0.0114	0.0018	8
37	0.2750	0.0012	296
38	0.3126	0.0009	461
39	0.2703	0.0007	506
40	0.1625	N/A*	N/A*
41	0.0351	0.0004	106
42	0.0023	0.0004	8

*C_{60} not detected, therefore sample is 100% $C_{60}O$.

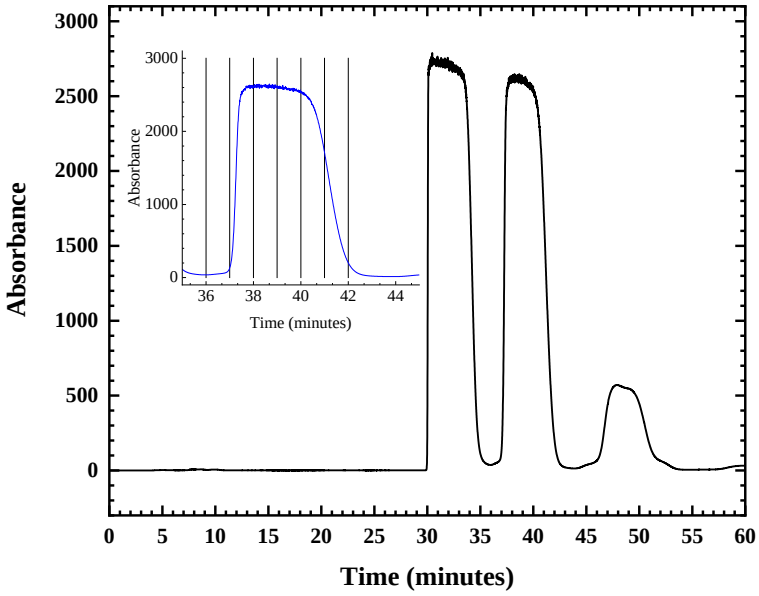

Figure 21: Example of a semi-preparative HPLC chromatogram, inset with extraction times intervals.

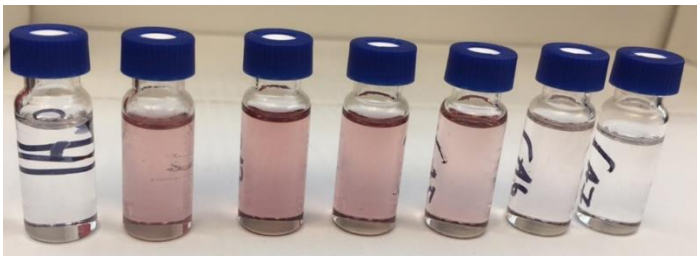

Figure 22: Extracted $C_{60}O$ fractions (36-42 minute fractions from left to right).

Figure 23 shows chromatograms of several re-analyzed fractions. As reported in Table 17, samples that contained a concentration ratio of $C_{60}O$:C_{60} greater than 100 could be used further. If any less, then it was simply stored in the fridge with the rest of the samples.

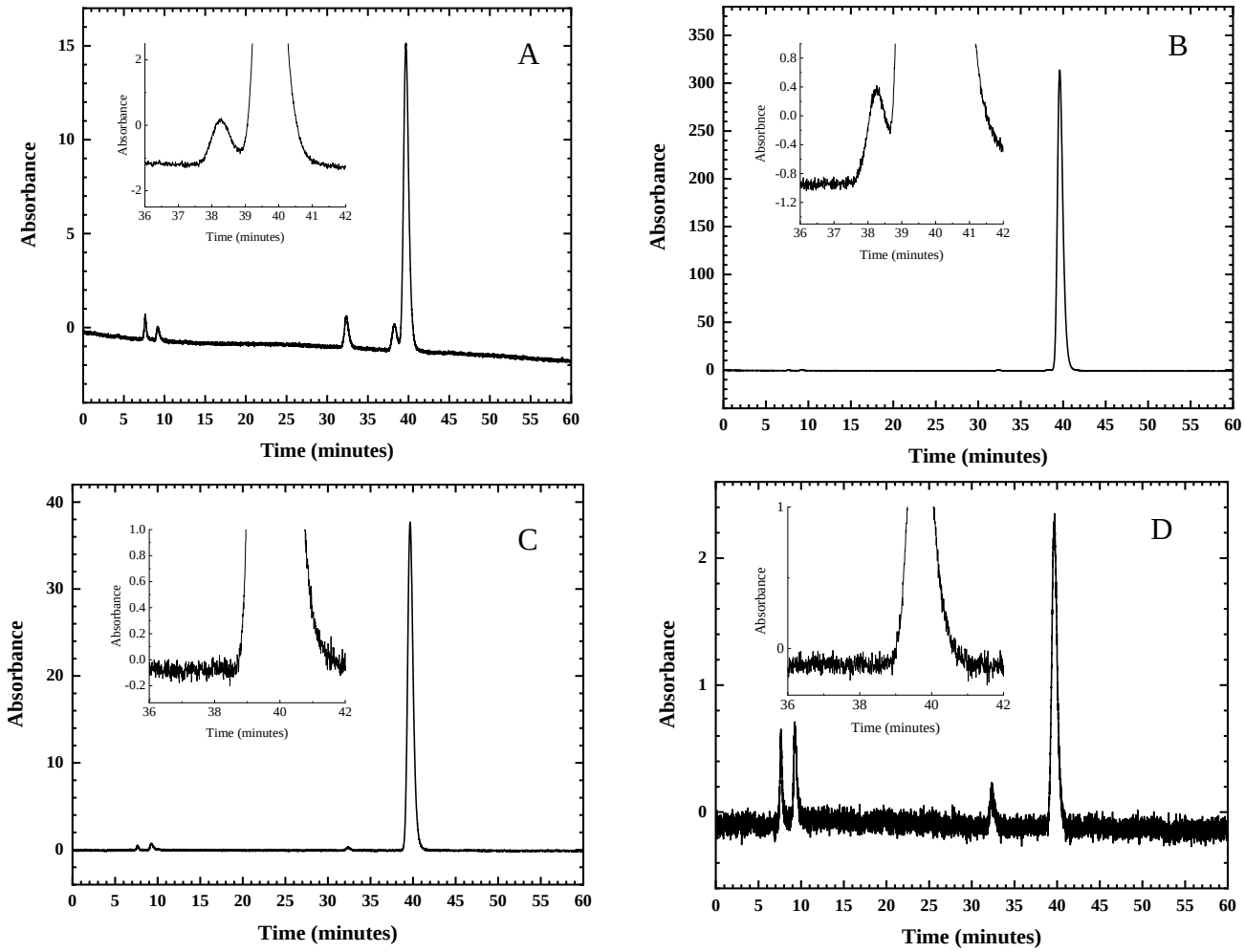

Figure 23: Re-analyzed HPLC chromatograms of extracted fractions, inset with $C_{60}O$ peak enlarged. (A) 36-minute fraction, (B) 37-minute fraction, (C) 41-minute fraction, and (D) 42-minute fraction.

3.5.1 – $C_{60}O$ and $C_{60}O_2$ Shoulder Peaks

$C_{60}O$ and $C_{60}O_2$ shoulder peaks were observed in concentrated samples of ozonated C_{60}. These shoulder peaks are clearly visible in chromatograms shown in Figure 23 B for $C_{60}O$ and Figure 24 for $C_{60}O_2$.

Solution phase ozonation of C_{60} generates an intermediate, $C_{60}O_3$, which is a [6,6]-closed ozone adduct known as [6,6]-closed ozonide.[15] Further dissociation of this intermediate species

via thermolysis and photolysis yields either [6,6]-closed epoxide or [5,6]-open oxidoannulene, respectively, as shown in Figure 2.[15,23]

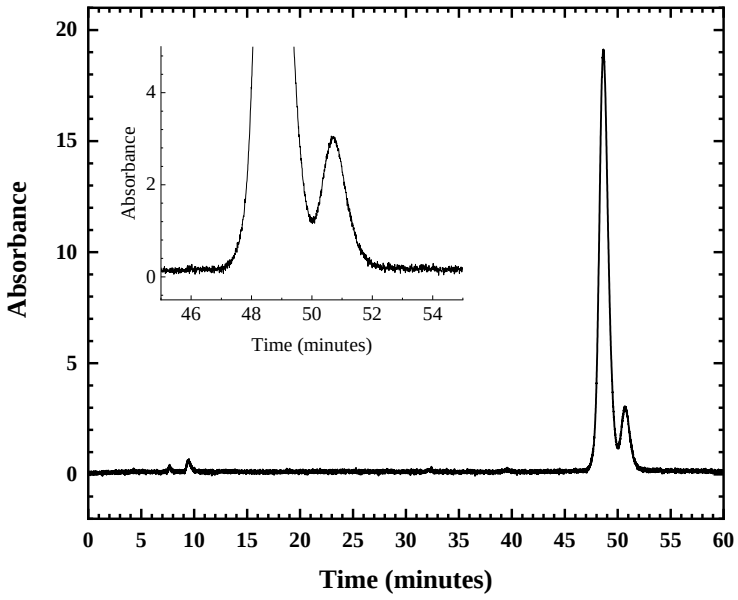

Figure 24: Re-analysis of an extracted fraction of $C_{60}O_2$, with inset showing enlarged $C_{60}O_2$ peak.

3.6 – Effect of Fluorescent Light and Dart Conditions on Ozonation

Additional ozonation experiments were carried out for further investigation of the shoulder peaks. These modified experiments were conducted after reviewing some previous research findings by Weisman, *et al.*[15] who described the promotion of the formation of the [5,6]-open oxidoannulene isomer, by ozonating a sample of C_{60} in darkness and separating $C_{60}O_3$ while shielding the sample from light using HPLC column cooled to 0 °C.[15] They have reported that several minutes of irradiation under a fluorescent desk lamp was sufficient to convert the chilled $C_{60}O_3$ fraction to [5,6]-open oxidoannulene isomer with a yield of nearly 100%.[15] A modified version of the experiment that was reported in Weisman, *et al*. was used, where the ozonation process of the sample was shielded, by foil, and performing under no laboratory lights. This

experiment was conducted as a preliminary study to determine if the composition of oxides will be affected by changing ambient light conditions at room temperature. Despite the experiment being performed using dark conditions, the resulting chromatogram and a re-analyzed fraction, at retention time of 37 minutes appeared to be similar to the results of the ambient light experiment shown in Figure 21 and Figure 23 B, where the compositions and the amount of oxides did not show a large difference.

The experiment conducted under fluorescence light yielded similar results as the ambient light experiments. The resulting chromatogram (Figure 25) and a re-analyzed fraction, at retention time of 37 minutes (Figure 26) appeared to be similar to the results of the ambient light experiment, where the compositions and the amount of oxides did not show a noteworthy difference. A comparison chromatogram is included in Appendix A. Due to both the shoulder and main $C_{60}O$ peaks being so close to each other, the compound in the shoulder peak was unable to be separated. Figure 27 shows a comparison of the various light condition sample, and is included in Appendix A.

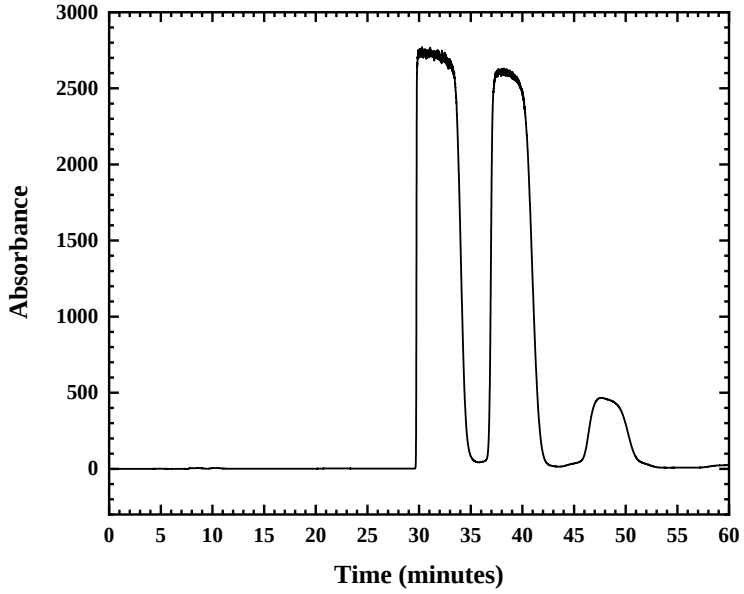

Figure 25: HPLC chromatogram from the experiment conducted under fluorescence light.

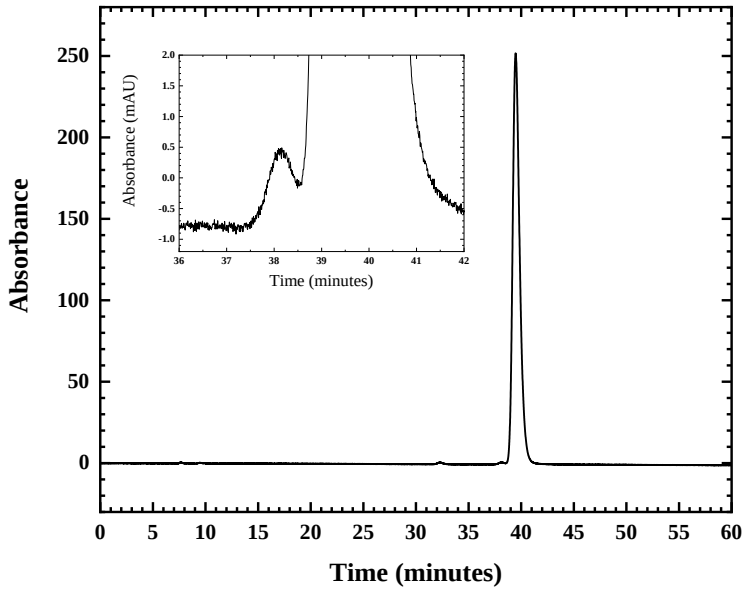

Figure 26: Re-analyzed $C_{60}O$ fraction, from the experiment conducted under fluorescence light, inset showing enlarged $C_{60}O$ peak.

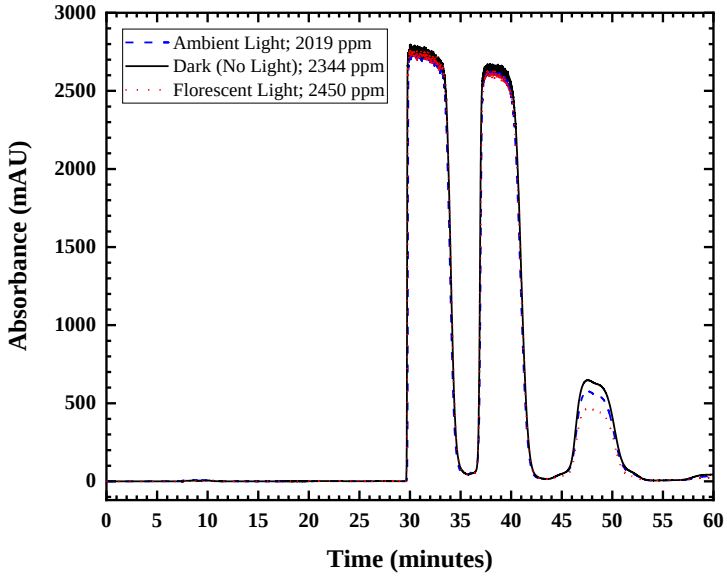

Figure 27: Comparison of various light condition samples.

3.7 – Optimization of Solvent Exchange from Toluene to Water to Produce Aqueous Suspensions of $C_{60}O$

As stated in Section 2.3.1, after evaporating toluene by rotary evaporation, dry $C_{60}O$ solid was stirred in nano pure water for about a month to achieve $C_{60}O$ colloids, as shown in Figure 28.

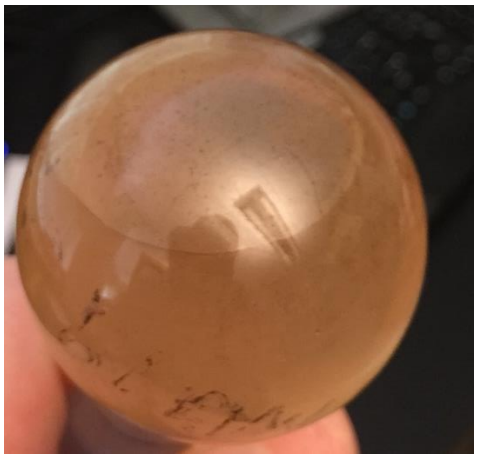

Figure 28: Sample of aqueous $C_{60}O$.

Stirring method was not effectively produced aqueous $C_{60}O$ samples, as it required a longer stirring period. As a modification, $C_{60}O$ solids were rotary evaporated with small amounts of ultrapure water to slowly evaporate off the toluene, in order to produce an aqueous sample. As the sample was dried, the aqueous $C_{60}O$ precipitated out of suspension, and adhered to the walls of the vial, as shown in Figure 29.

Figure 29: Unsuccessful solvent exchange.

We tested several modified versions of the solvent exchange process including different evaporation techniques to drive off the organic solvent and to find out the best set of conditions. Our expectation was to optimize the solvent exchange process where, the transfer of $C_{60}O$ from toluene to water could happen relatively slowly to avoid the precipitating out of the solution. Rotary evaporation combined with sonicator and shaker method yielded similar result as shown in Figure 30 where most of solid $C_{60}O$ was adhered to the walls of the flask.

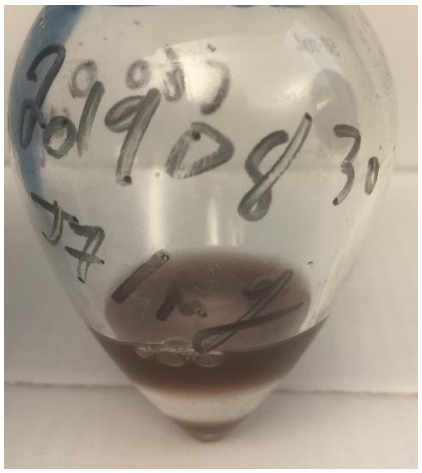

Figure 30: Condensed $C_{60}O$ sample with water.

The optimized method reported in Section 2.3.5 where samples were rotary evaporated and sonicated according to the parameters shown in Table 18 and Figure 31. During this process, pink (toluene) and clear (water) layers turned into a pale-yellow suspension after the organic solvent has fully evaporated (Figure 32). $C_{60}O$ in toluene is a nanoparticle solution with a characteristic purple-blue color and the $C_{60}O$ aggregates/clusters in aqueous phase would be responsible for a distinctive yellow-green color. The different colors are due to aggregation induced optical properties of C_{60} in solution.[26,27]

Table 18: Optimized rotary evaporator-sonicator parameters.

Rotary Evaporator Speed (RPM)	Sonicator Status	Sonicator Temperature (℃)	Vacuum Pressure (mmHg)	Amount of UPW Added (μL)	Approximate Sample Run Time (min)
280	On	RT	-457	6000	7 – 8

Figure 31: Sample being rotary evaporated and sonicated.

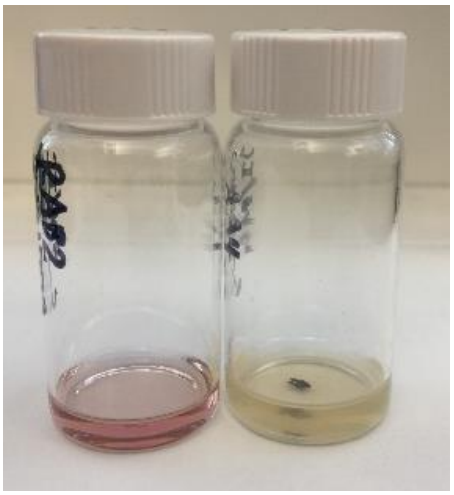

Figure 32: $C_{60}O$ solution in toluene (pink, left) and $C_{60}O$ aqueous colloids in water (yellow, right).

3.8 – HPLC analysis of Aqueous Colloids to Confirm the Presence of $C_{60}O$ in the Colloids

To determine the composition of the suspended particles, the aqueous samples were re-analyzed using HPLC. Figure 19 in Section 3.4 shows the original semi preparative chromatogram after ozonation. Figure 33 shows the re-analysis chromatogram of aqueous colloids. By the presence

of $C_{60}O$ peak in Figure 33, it is evident that the synthesized colloidal particles were entirely composed of $C_{60}O$.

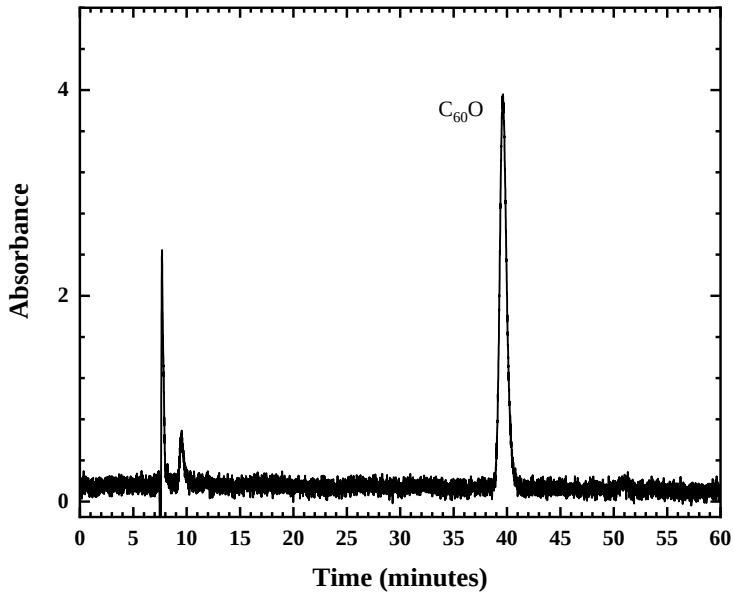

Figure 33: Confirmatory HPLC analysis of solvent exchanged *n*$C_{60}O$ sample.

3.9 – Characterization of Aqueous Colloidal Suspensions of $C_{60}O$

3.9.1 – Characterization by UV-Vis Spectroscopy

The aqueous colloidal suspensions of $C_{60}O$ were analyzed using UV-Vis spectroscopy, to confirm the maximum absorption wavelength. The experimental λ_{max} of $C_{60}O$ was determined to be 327 nm, as shown in Figure 34, which confirms the absorbance maxima reported in the literature.[14,15]

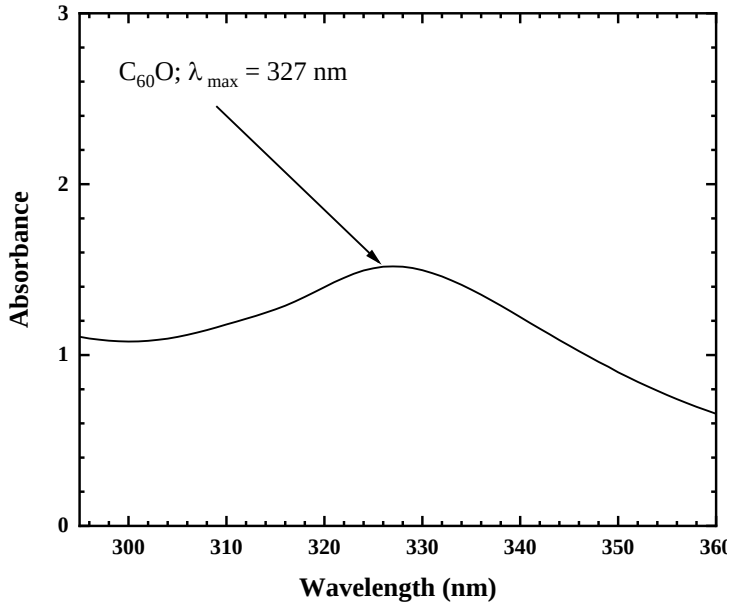

Figure 34: UV-vis absorbance spectrum of $C_{60}O$ colloids in toluene.

3.9.2 – Characterization by DLS

Average hydrodynamic diameter of suspended colloidal particles was determined to be 140 ± 20 nm, with a PDI of 0.28 ± 0.05, as shown in Figure 35. To the best of our knowledge, this is the first study that synthesized pure aqueous suspensions of $C_{60}O$. Comparatively, the size of these colloids is similar to the data that has been reported in literature, 139 nm, for aqueous C_{60} suspensions.[14]

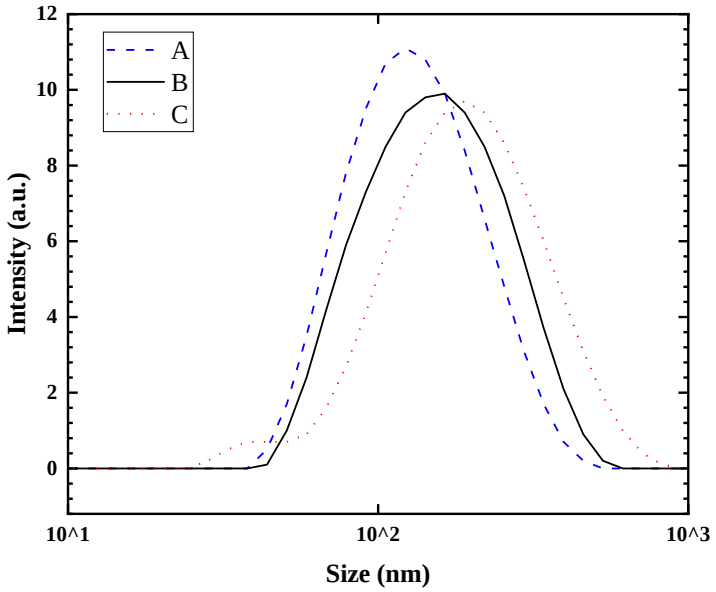

Figure 35: Average particle size for $n$$C_{60}$O.

CHAPTER FOUR: CONCLUSIONS AND FUTURE DIRECTIONS

4.1 – Conclusions

In the present study, fullerene oxides have successfully been synthesized by ozonating solutions of C_{60} in toluene under ambient conditions. Excellent separation between C_{60}, $C_{60}O$, and $C_{60}O_2$ was achieved using a mixture of toluene/n-hexane mobile phase in a Nacalai Cosmosil Buckyprep semi-preparative column. Separated compounds were successfully isolated and analyzed by UV-Vis spectroscopy. The wavelengths of maximum absorbance were determined to be 336, 328, and 315 nm for C_{60}, $C_{60}O$, and $C_{60}O_2$, respectively and are in agreement with literature reported values. Ultimately the successful synthesis of aqueous suspensions of $C_{60}O$, and the colloid composition was confirmed to be purely $C_{60}O$, by use of HPLC and UV-Vis analysis. Aqueous colloidal suspensions of $C_{60}O$ showed an average hydrodynamic diameter of 140 ± 20 nm, with a PDI of 0.28 ± 0.05. To the best of our knowledge, this is the first report of successful synthesis of aqueous colloidal suspensions of pure $C_{60}O$.

The current work successfully developed optimal conditions/methods to synthesize and separate $C_{60}O$, and to produce $C_{60}O$ aqueous colloidal suspensions. This would enable the investigation of the oxidative behavior of these suspensions and kinetic data analysis to elucidate mechanistic information. Furthermore, the probe-assisted oxidation monitoring approach will provide useful insight into other mechanistic studies.

4.2 – Future Directions

Future studies will focus on further characterization of aqueous colloidal suspensions of $C_{60}O$ using electron microscopy and determination of the surface zeta potential of the colloidal aggregates. Stability of these suspensions over time will be investigated by analyzing the

composition using HPLC. These colloidal suspensions and the developed optimal conditions/methods to synthesize $C_{60}O$ would enable us to investigate the oxidative behavior of these suspensions using probe-assisted spectroscopic determinations, such as fluorescence spectroscopy and sophisticated kinetic data analysis techniques to elucidate mechanistic information.

Further, the analysis of the shoulder peaks observed with each main peak of $C_{60}O$ and $C_{60}O_2$ in semi-preparative HPLC to determine the identity of those compounds will be explored. The ozonation procedure will be modified to maximize the amount of shoulder peak compound and the HPLC separation procedure will be optimized to achieve a better separation between main HPLC peak and the shoulder peak. These future experiments will aid in the determination of the mechanisms that drive these oxidation reactions in fullerenes, which will enable the determination of the environmental toxicity of these compounds and designing environmentally friendly waste disposal methods for fullerenes.

REFERENCES

(1) The Nobel Prize in Chemistry 1996 Press Release. 1996.

(2) Tiwari, A. J.; Morris, J. R.; Vejerano, E. P.; Hochella, M. F.; Marr, L. C. Oxidation of C_{60} Aerosols by Atmospherically Relevant Levels of O_3. *Environ. Sci. Technol.* **2014**, *48* (5), 2706–2714.

(3) Buckminsterfullerene. *National Center for Biotechnology Information. PubChem Compound Database.*

(4) Murayama, H.; Tomonoh, S.; Alford, J. M.; Karpuk, M. E. Fullerene Production in Tons and More: From Science to Industry. *Fullerenes Nanotub. Carbon Nanostructures* **2004**, *12* (2), 1–9.

(5) Kroto, H. W.; Heath, J. R.; O'Brien, S. C.; Curl, R. F.; Smalley, R. E. C_{60}: Buckminsterfullerene. *Nature* **1985**, *318* (6042), 162–163.

(6) Krätschmer, W.; Lamb, L. D.; Fostiropoulos, K.; Huffman, D. R. Solid C_{60}: A New Form of Carbon. *Nature* **1990**, *347*, 354–358.

(7) Chibante, L. P. F.; Heymann, D. On the Geochemistry of Fullerenes: Stability of C_{60} in Ambient Air and the Role of Ozone. *Geochim. Cosmochim. Acta* **1993**, *57*, 1879–1881.

(8) Colvin, V. L. The Potential Environmental Impact of Engineered Nanomaterials. *Nat. Biotechnol.* **2003**, *22* (10), 1166–1170.

(9) Ruoff, R. S.; Tse, D. S.; Malhotra, R.; Lorents, D. C. Solubility of C_{60} in a Variety of Solvents. *J. Phys. Chem.* **1993**, *97* (13), 3379–3383.

(10) Heymann, D. Solubility of C_{60} in Alcohols and Alkanes. *Carbon N. Y.* **1996**, *34* (5), 627–631.

(11) Andrievsky, G. V.; Kosevich, M. V.; Vovk, O. M.; Shelkovsky, V. S.; Vashchenko, L. A. On the Production of an Aqueous Colloidal Solution of Fullerenes. *J. Chem. Soc. Chem. Commun.* **1995**, 1281–1282.

(12) Pelletier, M.; Bottero, J. -Y.; Brant, J.; Thill, A.; Labille, J.; Wiesner, M.; Masion, A.; Villiéras, F.; Rose, J. Affinity of C_{60} Fullerenes with Water. *Fullerenes, Nanotub. Carbon Nanostructures* **2006**, *14*, 307–314.

(13) Fortner, J. D.; Lyon, D. Y.; Sayes, C. M.; Boyd, A. M.; Falkner, J. C.; Hotze, E. M.; Alemany, L. B.; Tao, Y. J.; Guo, W.; Ausman, K. D.; Colvin, V. L.; Hughes, J. B. C_{60} in Water: Nanocrystal Formation and Microbial Response. *Environ. Sci. Technol.* **2005**, *39*, 4307–4316.

(14) Murdianti, B. S.; Damron, J. T.; Hilburn, M. E.; Maples, R. D.; Hikkaduwa Koralege, R. S.; Kuriyavar, S. I.; Ausman, K. D. C_{60} Oxide as a Key Component of Aqueous C_{60} Colloidal Suspensions. *Environ. Sci. Technol.* **2012**, *46* (14), 7446–7453.

(15) Weisman, R. B.; Heymann, D.; Bachilo, S. M. Synthesis and Characterization of the "Missing" Oxide of C_{60}: [5,6]-Open $C_{60}O$. *J. Am. Chem. Soc.* **2001**, *123* (39), 9720–9721.

(16) Maples, R. D.; Hilburn, M. E.; Murdianti, B. S.; Hikkaduwa Koralege, R. S.; Williams, J. S.; Kuriyavar, S. I.; Ausman, K. D. Optimized Solvent-Exchange Synthesis Method for C_{60} Colloidal Dispersions. *J. Colloid Interface Sci.* **2012**, *370* (1), 27–31.

(17) Johnston, H. J.; Hutchison, G. R.; Christensen, F. M.; Aschberger, K.; Stone, V. The Biological Mechanisms and Physicochemical Characteristics Responsible for Driving Fullerene Toxicity. *Toxicol. Sci.* **2010**, *114* (2), 162–182.

(18) Aschberger, K.; Johnston, H. J.; Stone, V.; Aitken, R. J.; Tran, C. L.; Hankin, S. M.; Peters, S. A. K.; Christensen, F. M. Review of Fullerene Toxicity and Exposure – Appraisal of a

Human Health Risk Assessment, Based on Open Literature. *Regul. Toxicol. Pharmacol.* **2010**, *58*, 455–473.

(19) Oberdörster, E. Manufactured Nanomaterials (Fullerenes, C_{60}) Induce Oxidative Stress in the Brain of Juvenile Largemouth Bass. *Environ. Health Perspect.* **2004**, *112* (10), 1058–1062.

(20) Sayes, C. M.; Gobin, A. M.; Ausman, K. D.; Mendez, J.; West, J. L.; Colvin, V. L. Nano-C_{60} Cytotoxicity Is Due to Lipid Peroxidation. *Biomaterials* **2005**, *26* (36), 7587–7595.

(21) Nikolic, Z.; Dramicanin, M.; Raicevic, N.; Todorovic-Markovic, B.; Vranjes-Djuric, S.; Isakovic, A.; Markovic, Z.; Mirkovic, M.; Harhaji, L.; Nikolic, N.; Trajkovic, V. Distinct Cytotoxic Mechanisms of Pristine versus Hydroxylated Fullerene. *Toxicol. Sci.* **2006**, *91* (1), 173–183.

(22) Sayes, C. M.; Fortner, J. D.; Guo, W.; Lyon, D.; Boyd, A. M.; Ausman, K. D.; Tao, Y. J.; Sitharaman, B.; Wilson, L. J.; Hughes, J. B.; West, J. L.; Colvin, V. L. The Differential Cytotoxicity of Water-Soluble Fullerenes. *Nano Lett.* **2004**, *4* (10), 1881–1887.

(23) Heymann, D.; Bachilo, S. M.; Weisman, R. B.; Cataldo, F.; Fokkens, R. H.; Nibbering, N. M. M.; Vis, R. D.; Chibante, L. P. F. $C_{60}O_3$, a Fullerene Ozonide: Synthesis and Dissociation to $C_{60}O$ and O_2. *J. Am. Chem. Soc.* **2000**, *122* (46), 11473–11479.

(24) Jiang, S.; Duan, S.; Liu, K.; Yang, X.; Cheng, C.; Li, J.; Wang, G.; Wang, G. Highly Efficient Synthesis of [60] Fullerene Oxides by Plasma Jet. *R. Soc. Open Sci.* **2017**, *4* (9), 1–9.

(25) Heymann, D. Ozonides and Oxides of C_{60} and C_{70}: A Review. *Fullerenes Nanotub. Carbon Nanostructures* **2004**, *12* (4), 715–729.

(26) Zhang, F.; Zhang, X. Solvent-Induced Optical Properties of C_{60}. *J. Lumin.* **2010**, *130* (5),

787–791.

(27) Saraswati, T. E.; Setiawan, U. H.; Ihsan, M. R.; Isnaeni, I.; Herbani, Y. The Study of the Optical Properties of C_{60} Fullerene in Different Organic Solvents. *Open Chem.* **2019**, *17*, 1198–1212.

(28) Teprovich, J.; Washington, A.; Dixon, J.; Ward, P.; Christian, J.; Peters, B.; Zhou, J.; Giri, S.; Sharp, D.; Velten, J.; Compton, R.; Jena, P.; Zidan, R. Investigation of Hydrogen Induced Fluorescence in C_{60} and Its Potential Use in Luminescence Down Shifting Applications. *Nanoscale* **2016**, *8* (44), 18760–18770.

(29) Snyder, L.; Kirkland, J.; Dolan, J. *Introduction to Modern Liquid Chromatography*, 3rd ed.; John Wiley & Sons, Inc.: Hoboken, NJ, 2010.

APPENDIX A: EXPERIMENTAL METHODS CHROMATOGRAMS

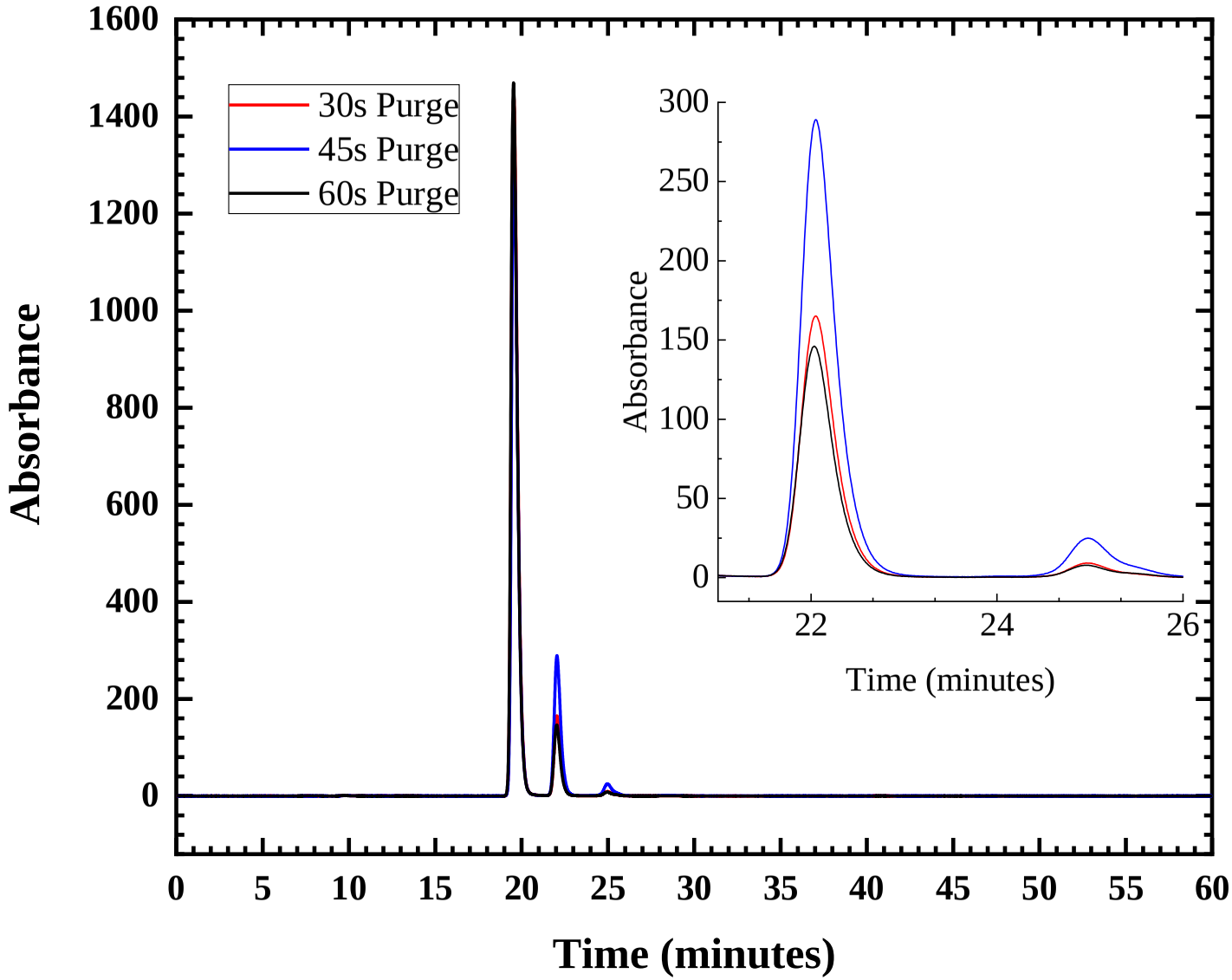

Figure A1: 100 µL Injection of combined 406 ppm samples with 30 s, 45 s, and 60 s purge times, a generator setting of 2, using a mobile phase of 100% toluene.

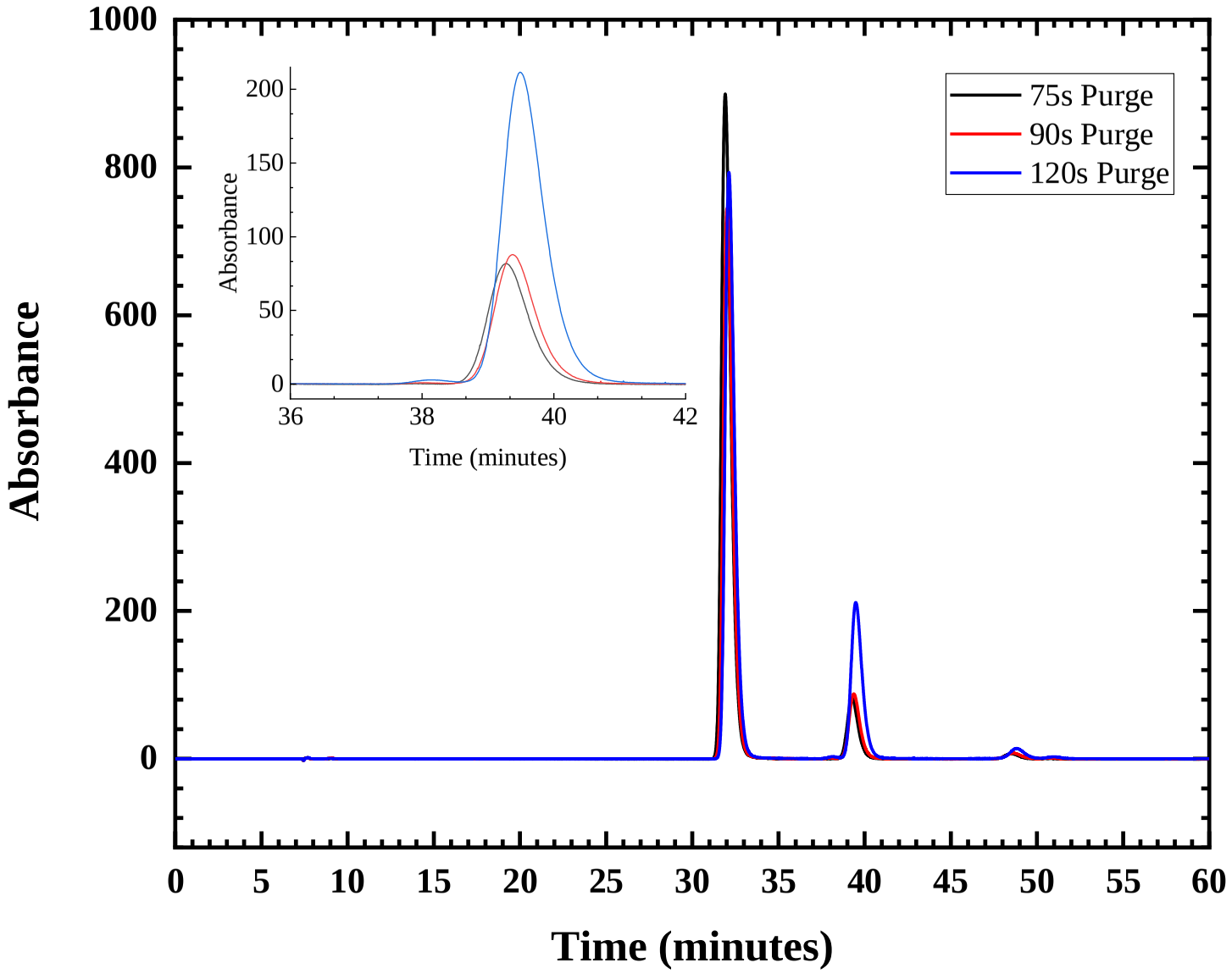

Figure A2: 100 µL Injection of combined 406 ppm samples with 75 s, 90 s, and 120 s purge times, a generator setting of 2, using a mobile phase of toluene/n-hexane (70:30).

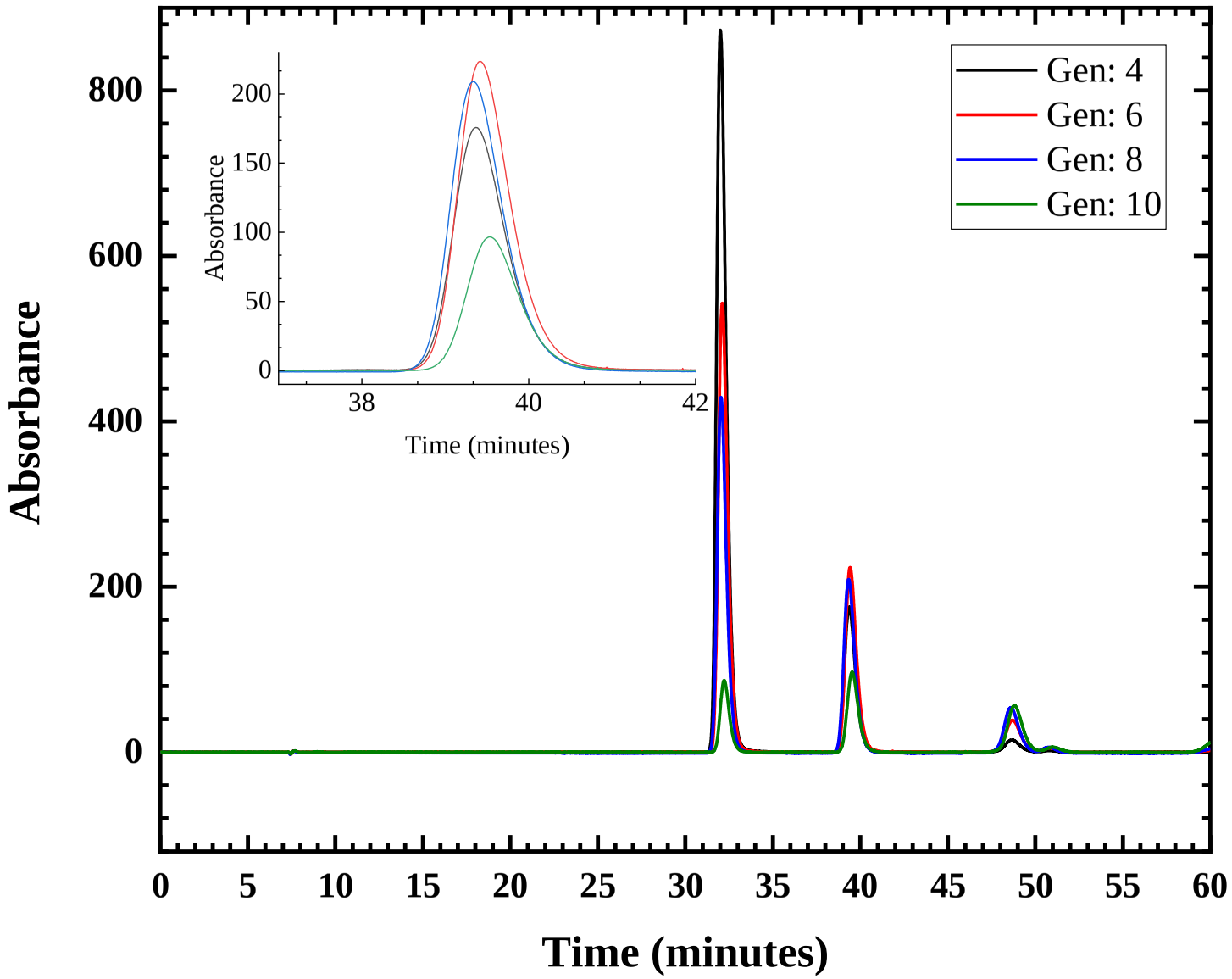

Figure A3: 100 µL Injection of a 404 ppm sample, with a purge of 120 s, generator setting of 4, 6, 8, and 10, using a mobile phase of toluene/n-hexane (70:30).

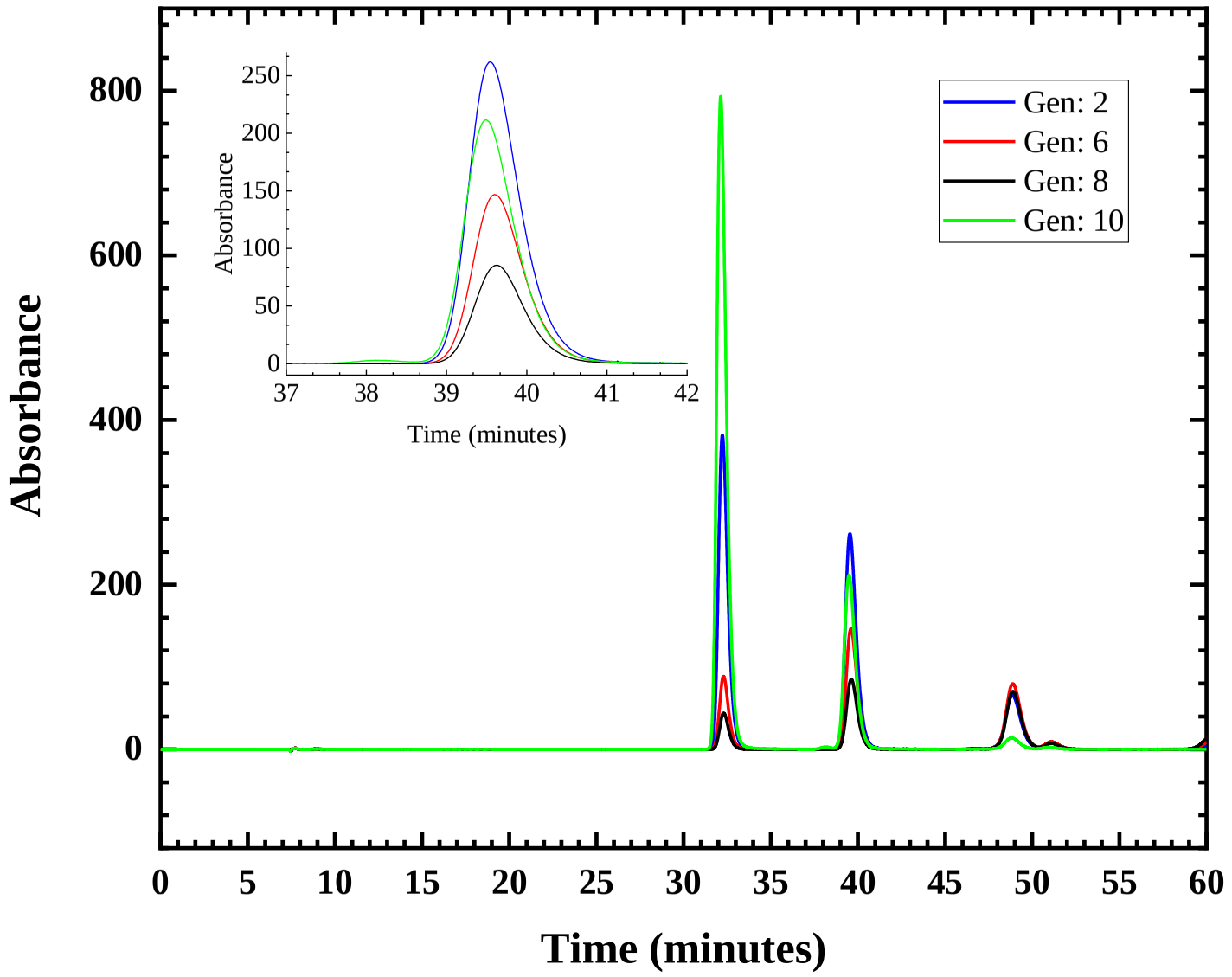

Figure A4: 100 µL Injection of a 404 ppm sample, with a purge of 120 s, generator setting of 2, 4, 8, and 10, using a mobile phase of toluene/n-hexane (70:30).

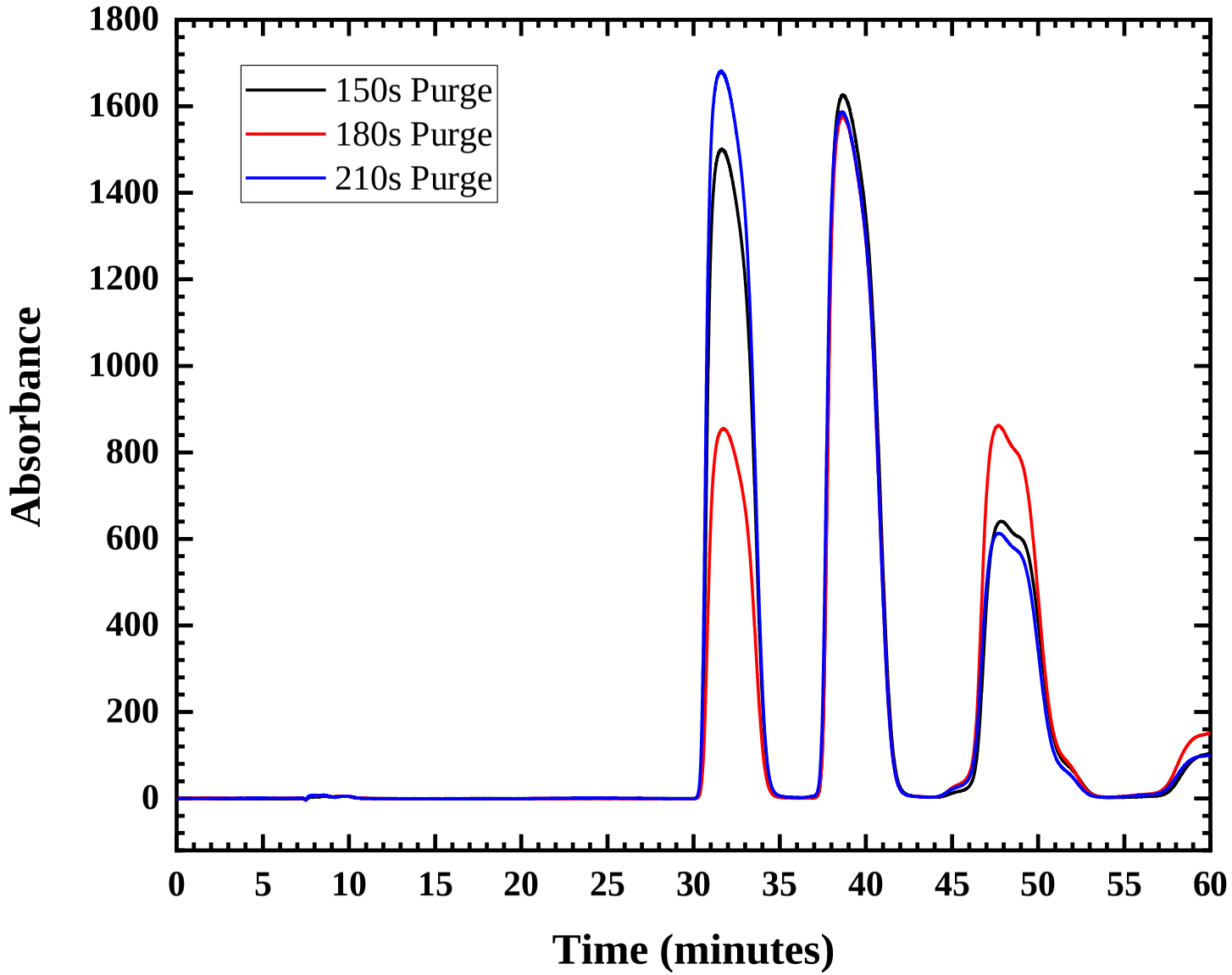

Figure A5: 2500 µL Injection of a 403 ppm sample, with a purge of 150 s, 180 s, and 210 s, with a generator setting of 6, using a mobile phase of toluene/n-hexane (70:30).

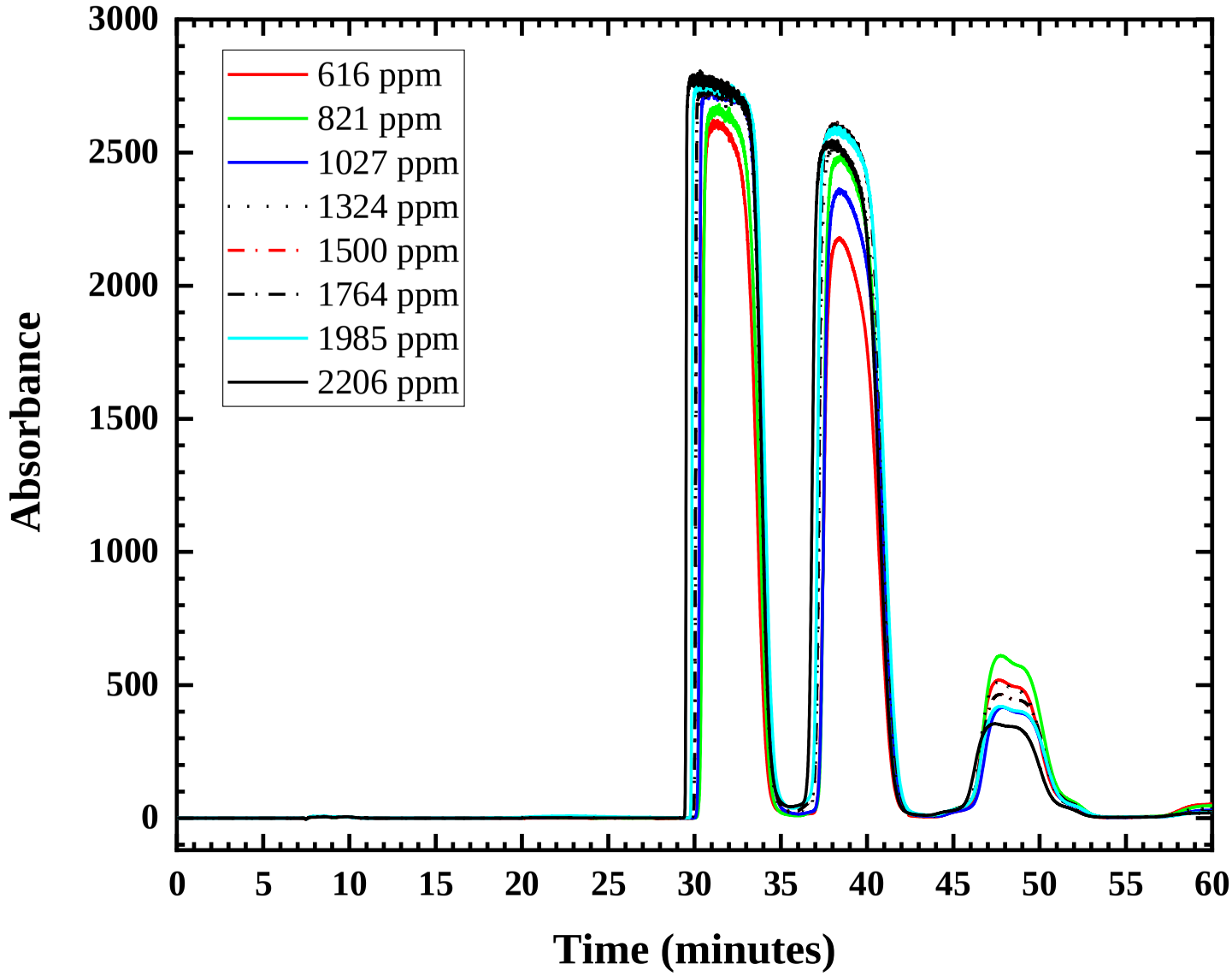

Figure A6: 2500 µL Injections of various concentrations of samples, with a purge of 120 s, and a generator setting of 6.

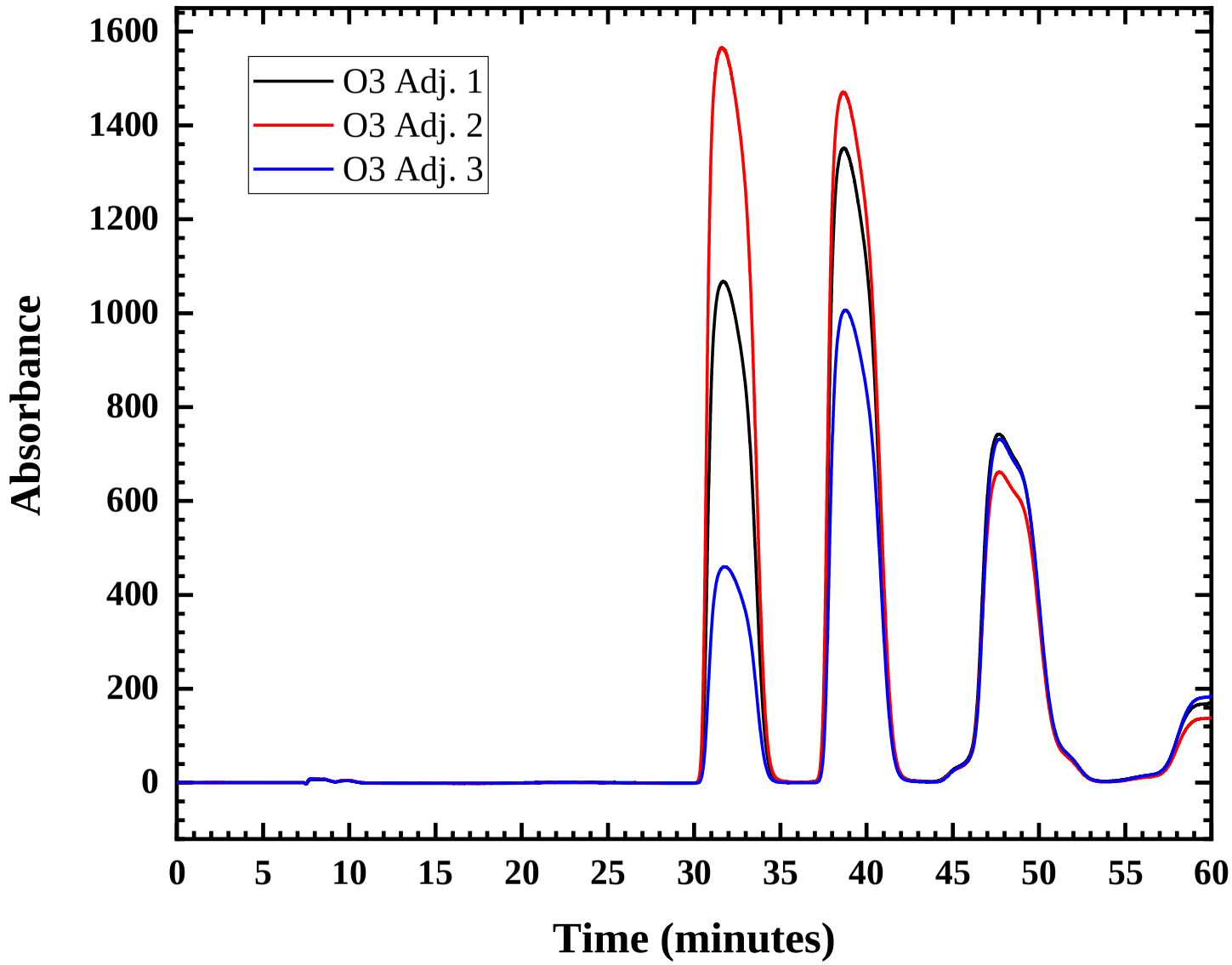

Figure A7: 2500 µL Injection of a 403 ppm sample, with a purge of 120 s, with a generator setting of 6, using the adjusted parameters 1, 2, and 3, using a mobile phase of toluene/n-hexane (70:30).

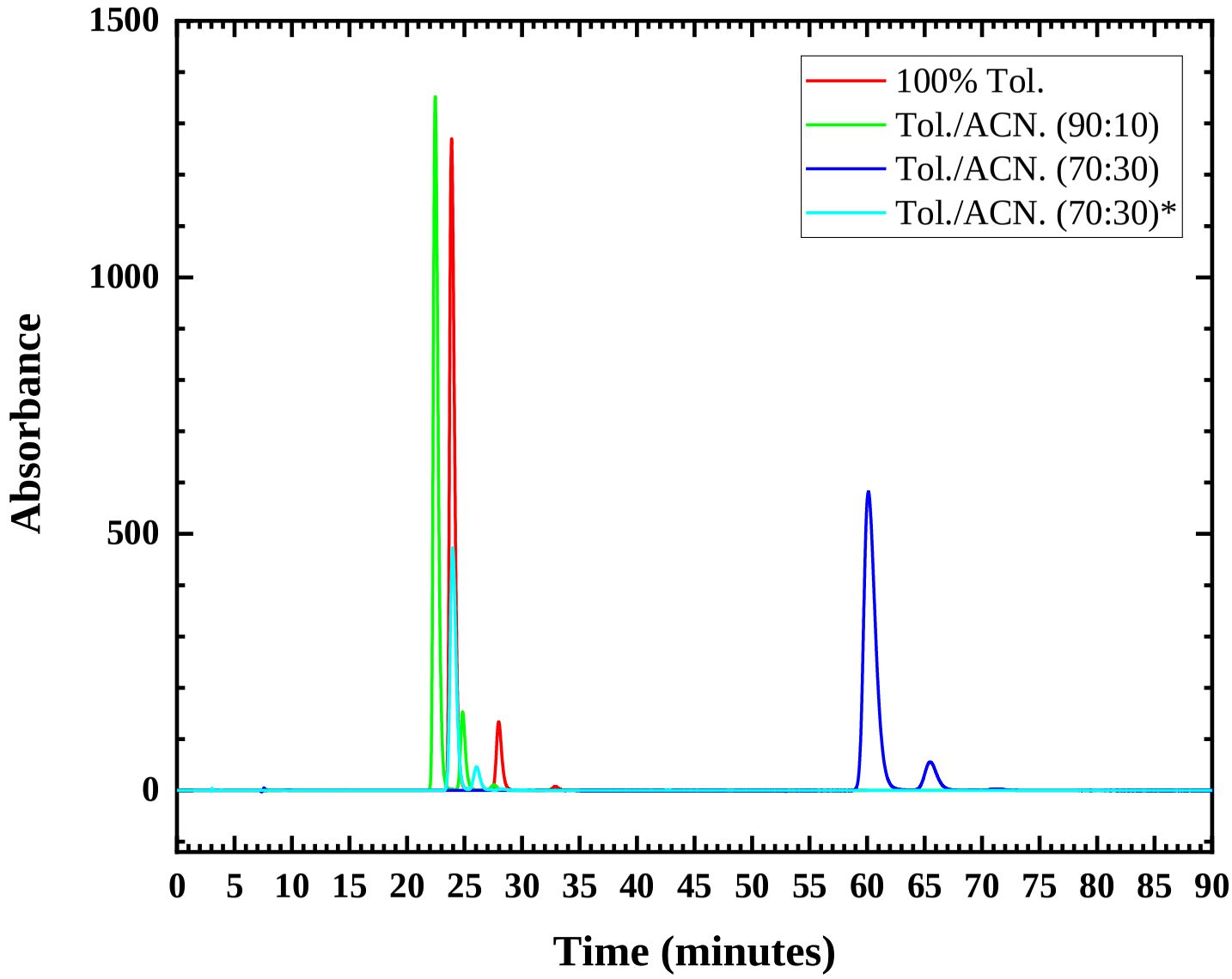

Figure A8: 100 µL Injection of a 406 ppm sample, using various mobile phase mixtures of toluene (Tol.) and acetonitrile (ACN.) using a flow rate of 2.000 mL/min. *Used a flow rate of 5.000 mL/min.

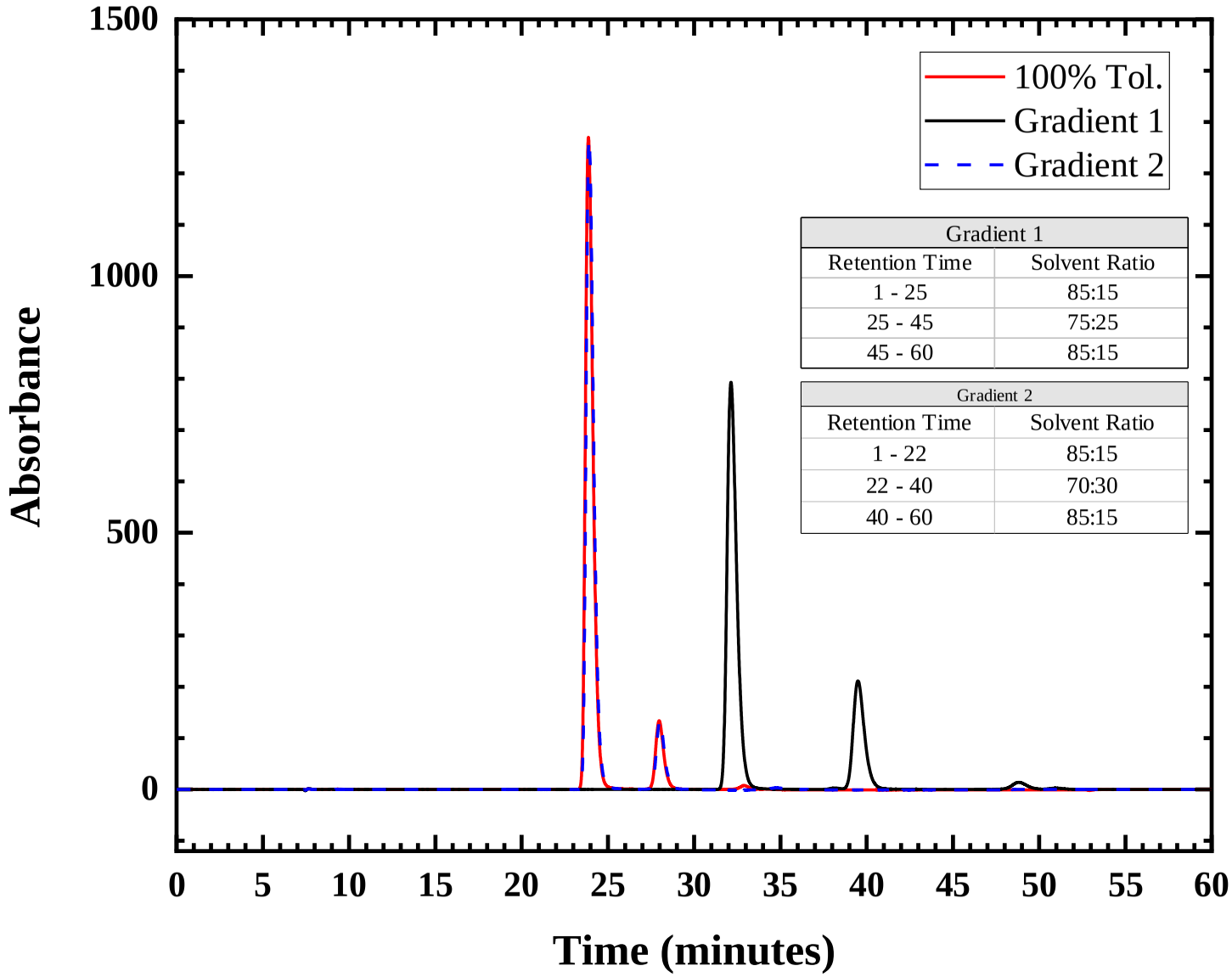

Figure A9: 100 µL Injection of a 406 ppm sample, using various gradient mobile phase mixtures of toluene and n-hexane (i.e. 85:15), using a flow rate of 2.000 mL/min.

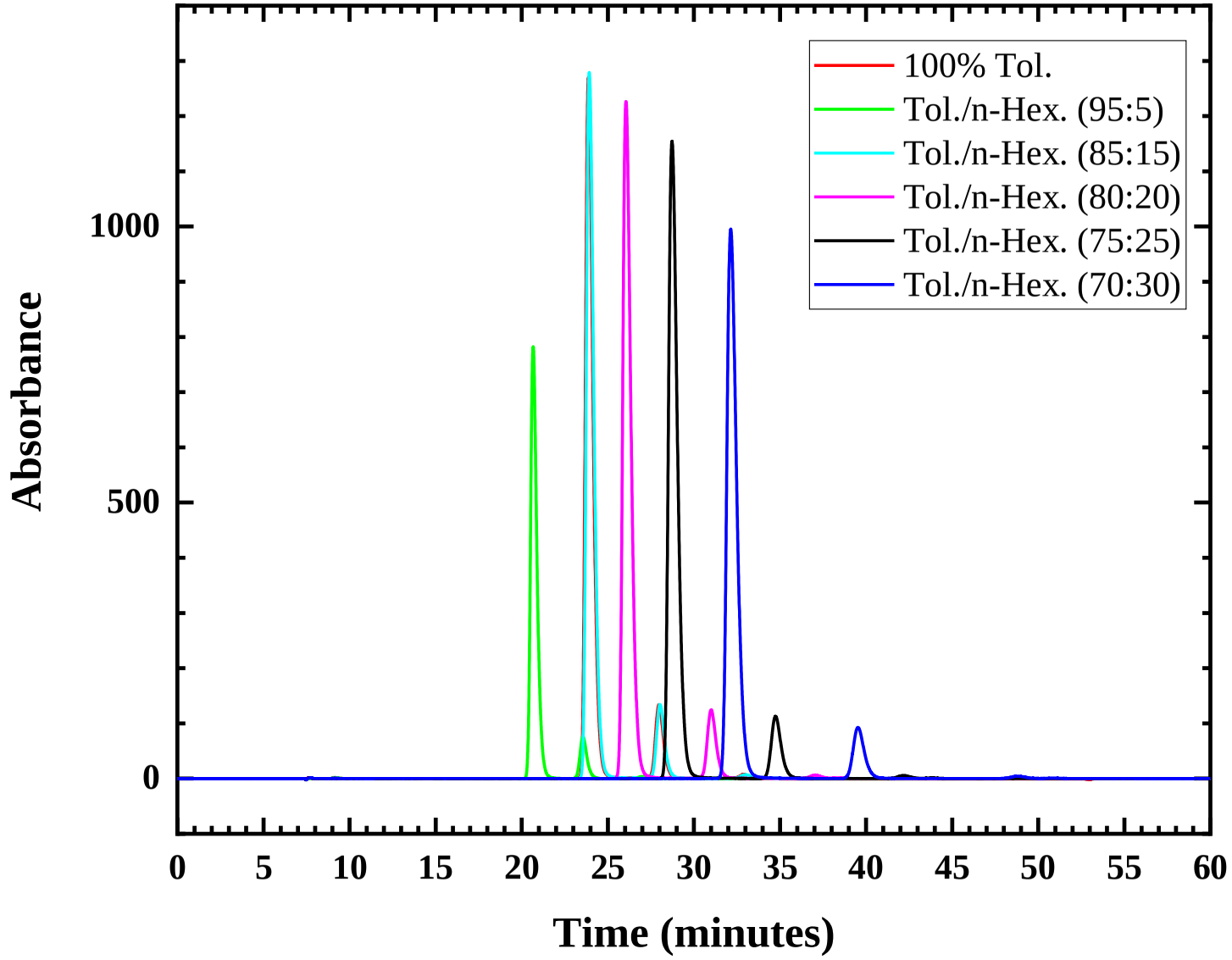

Figure A10: 100 µL Injection of a 406 ppm sample, using a mobile phase of toluene (Tol.) and n-hexane (n-Hex.) (70:30), and a flow rate of 2.000 mL/min.

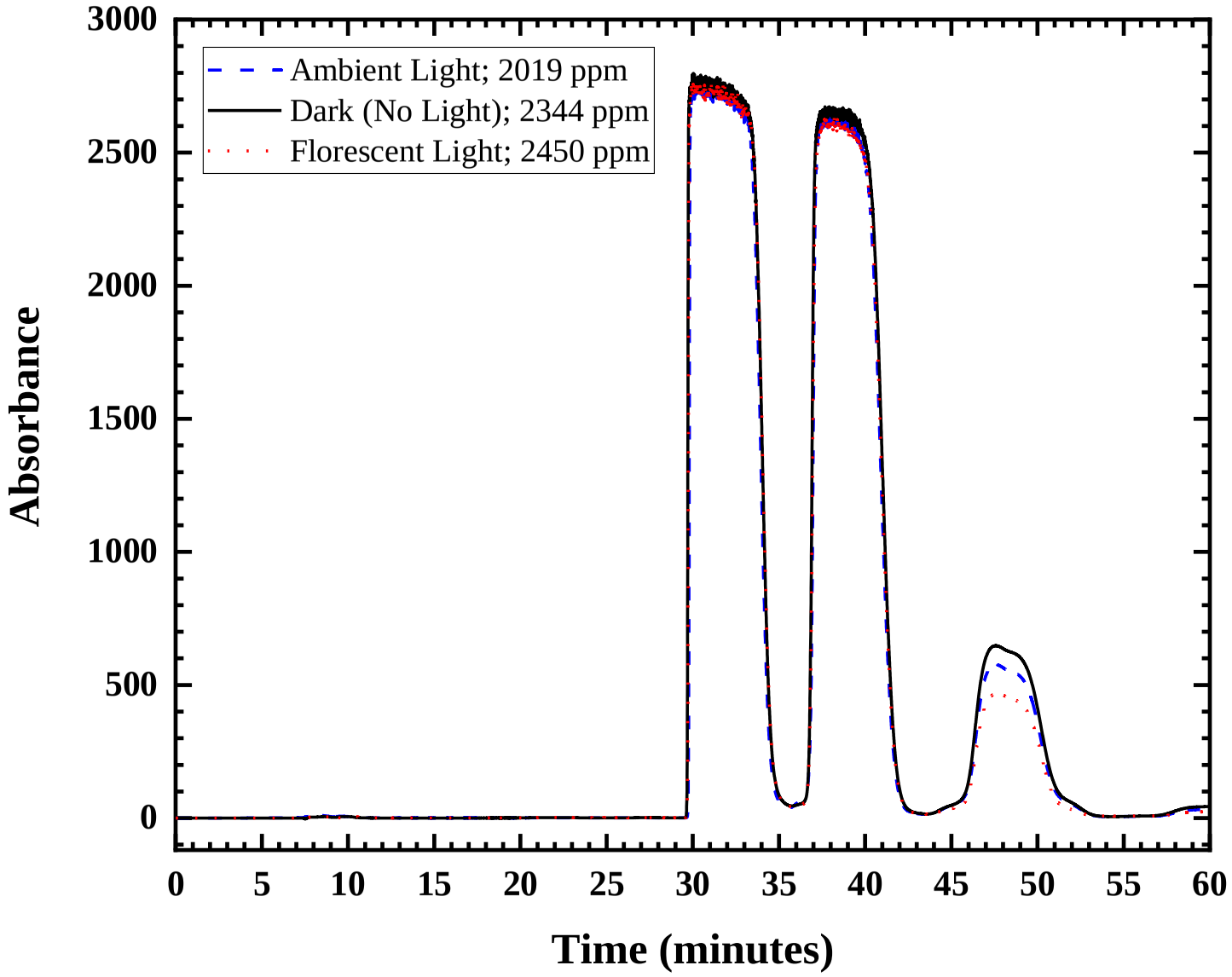

Figure A11: 2500 µL Injection of Various light condition samples, using a mobile phase of toluene/n-hexane (70:30), and a flow rate of 2.000 mL/min.

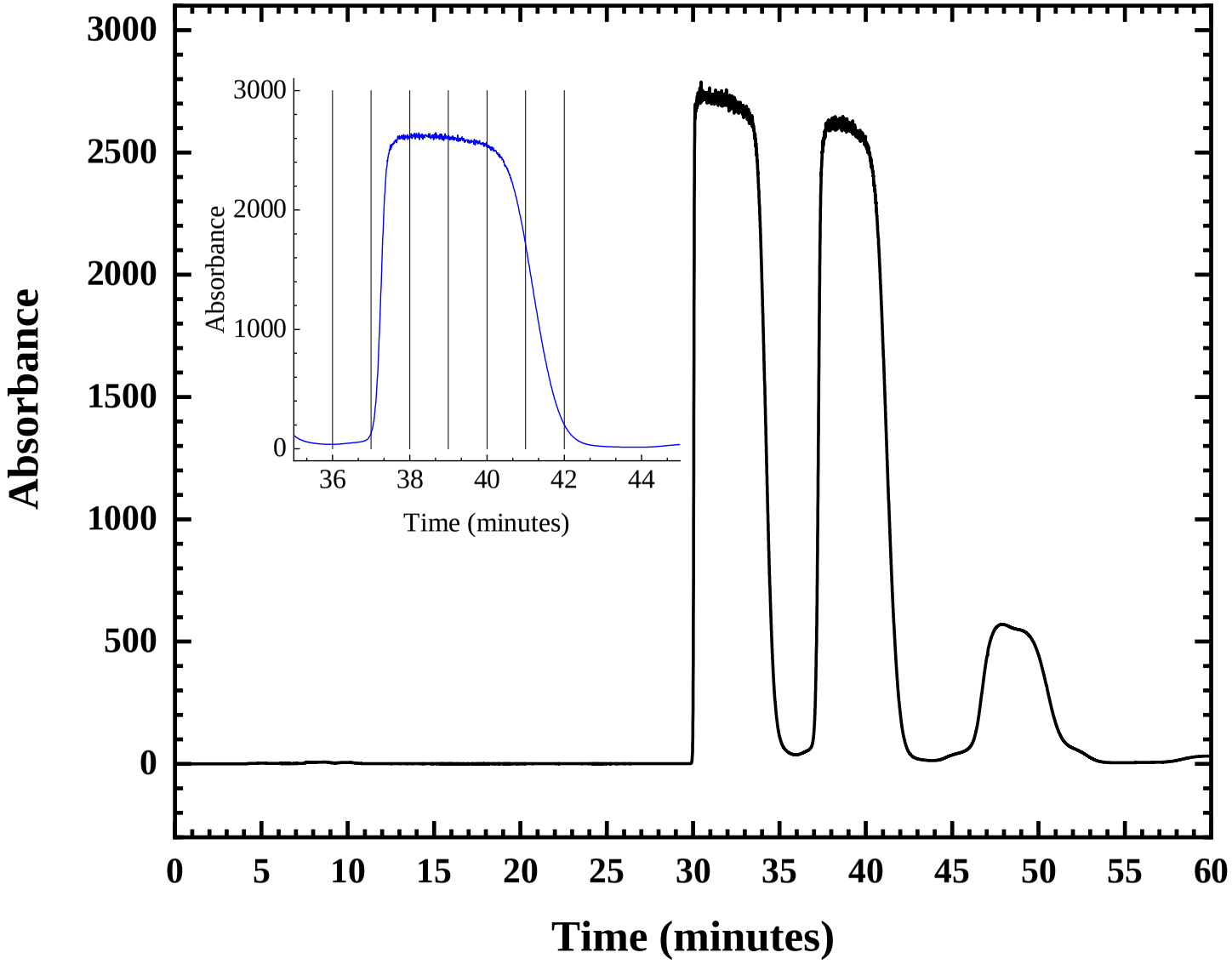

Figure A12: Ambient light experiment, with a 2500 µL injection of a 2019 ppm sample, using a mobile phase of toluene/n-hexane (70:30), and a flow rate of 2.000 mL/min, with an enlarged tile highlighting the fraction extractions.

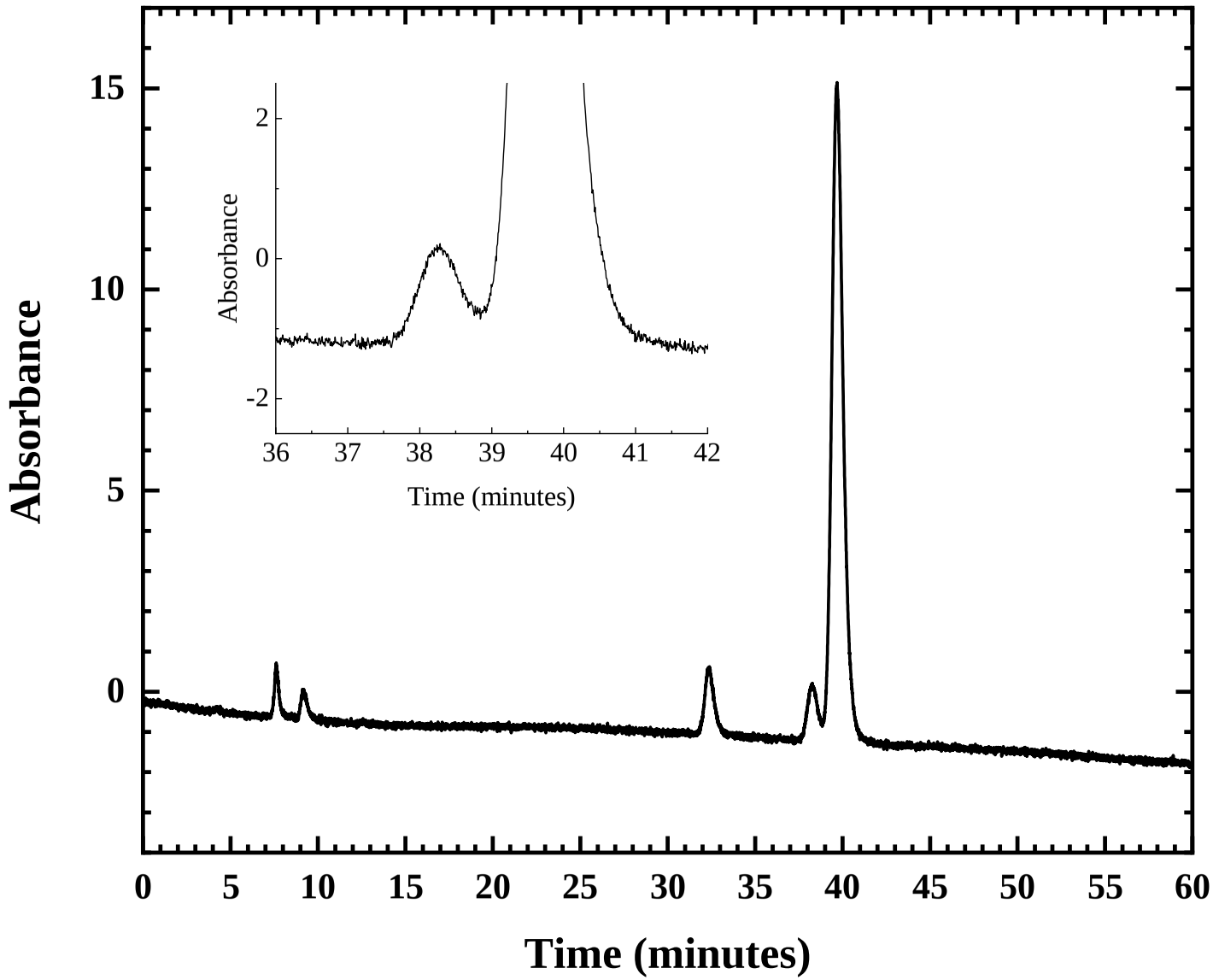

Figure A13: Re-analysis of an extracted fraction at a retention time of 36 minutes using a 100 µL injection, a mobile phase of toluene/n-hexane (70:30), and a flow rate of 2.000 mL/min.

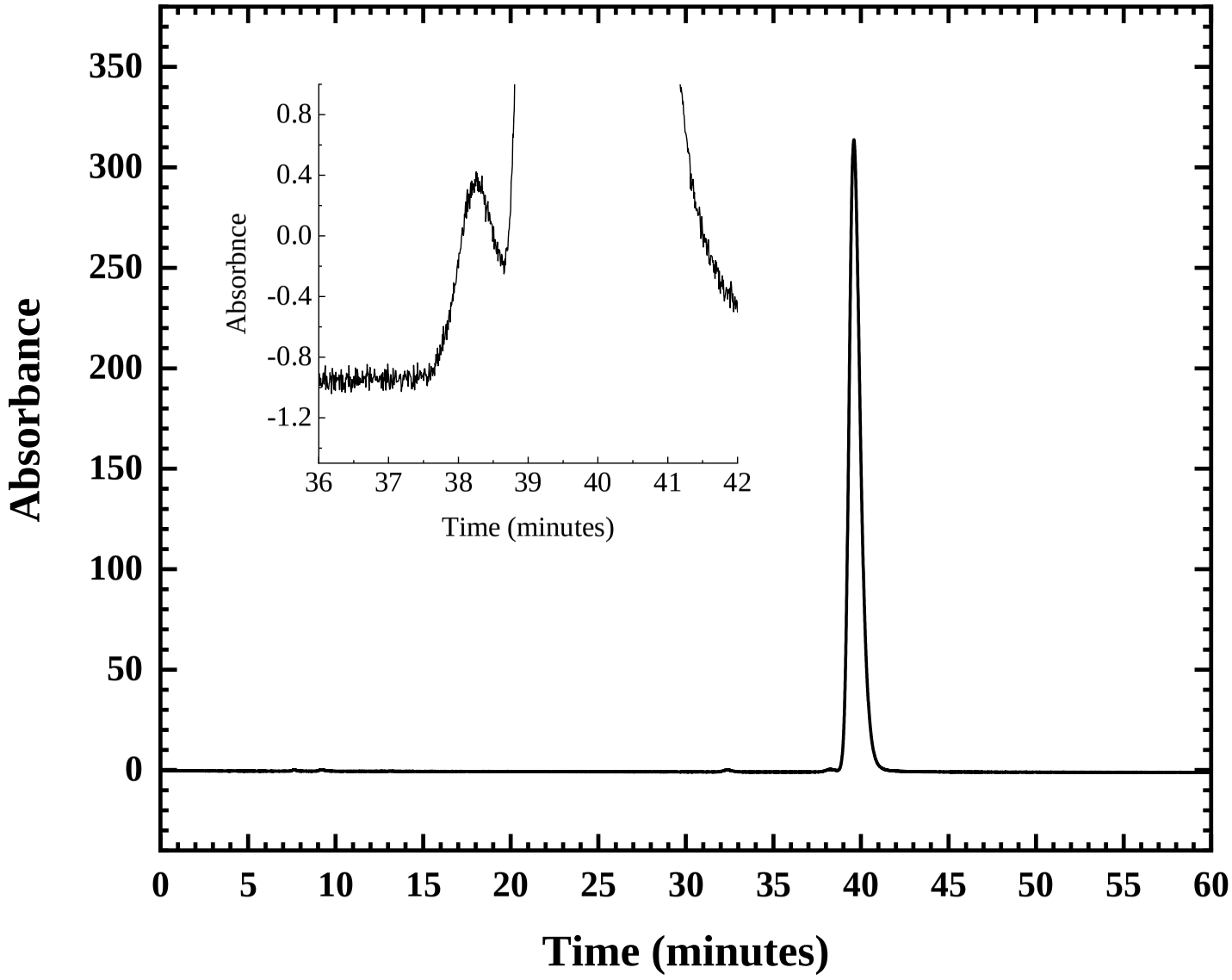

Figure A14: Re-analysis of an extracted fraction at a retention time of 37 minutes using a 100 µL injection, a mobile phase of toluene/n-hexane (70:30), and a flow rate of 2.000 mL/min.

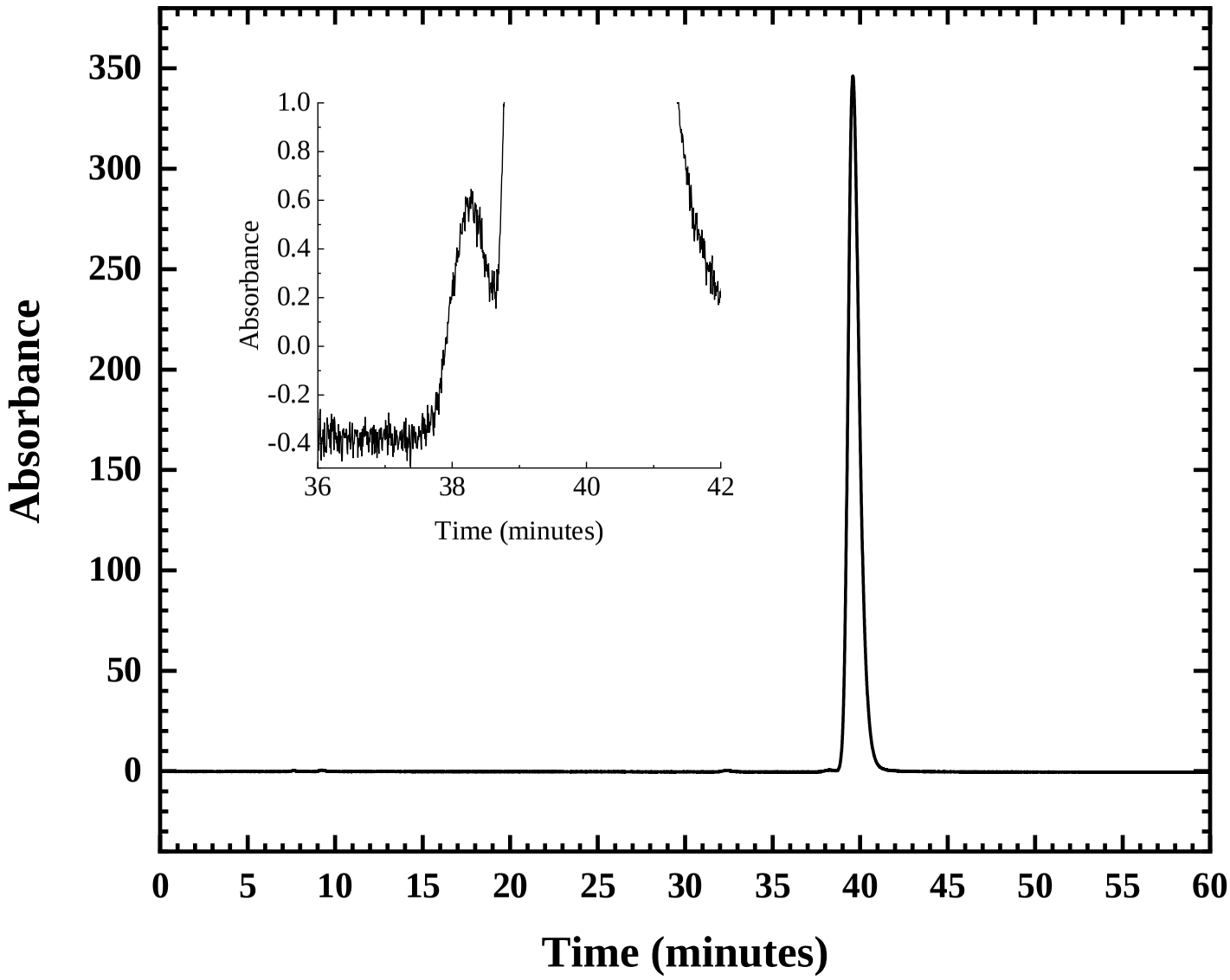

Figure A15: Re-analysis of an extracted fraction at a retention time of 38 minutes using a 100 µL injection, a mobile phase of toluene/n-hexane (70:30), and a flow rate of 2.000 mL/min.

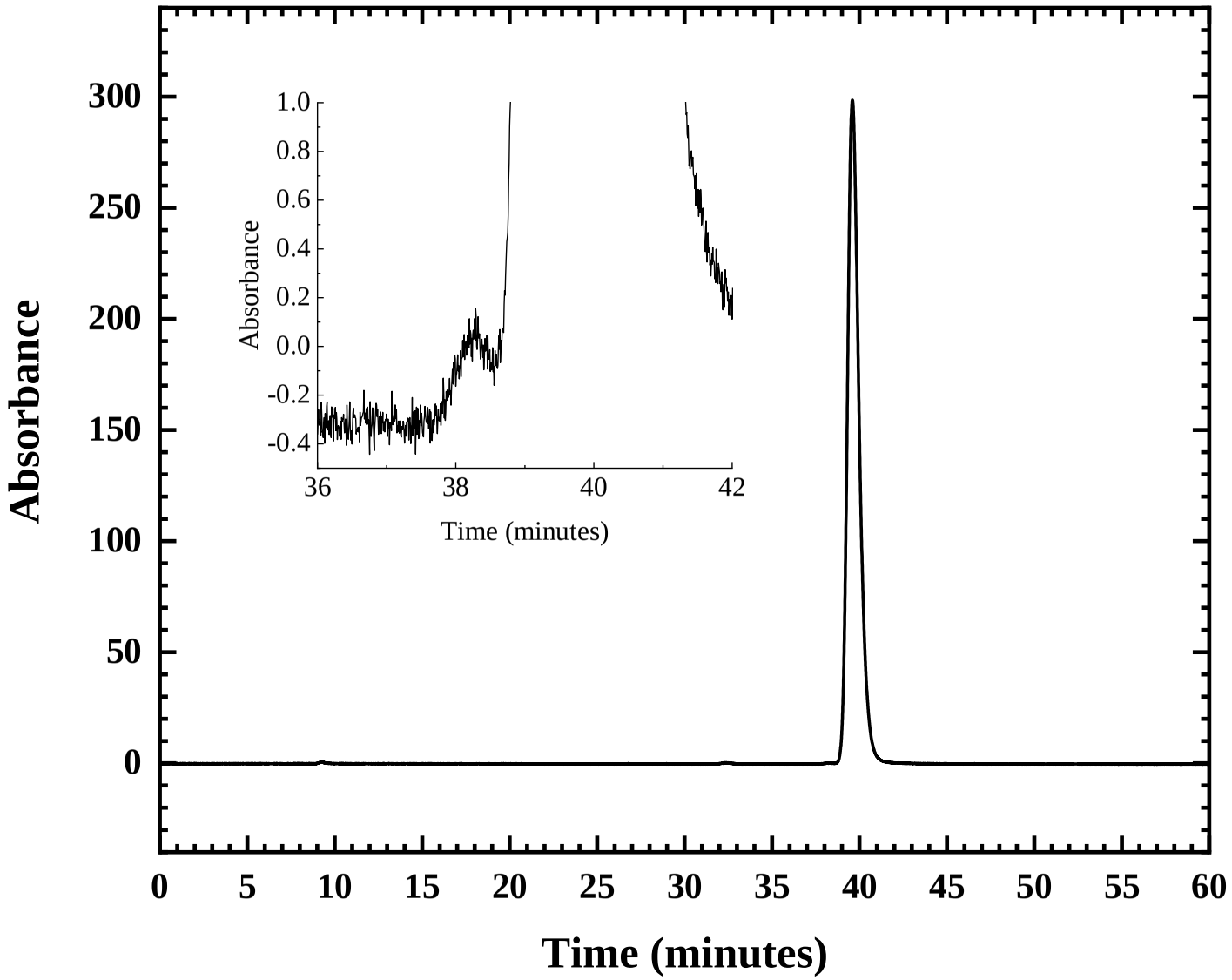

Figure A16: Re-analysis of an extracted fraction at a retention time of 39 minutes using a 100 µL injection, a mobile phase of toluene/n-hexane (70:30), and a flow rate of 2.000 mL/min.

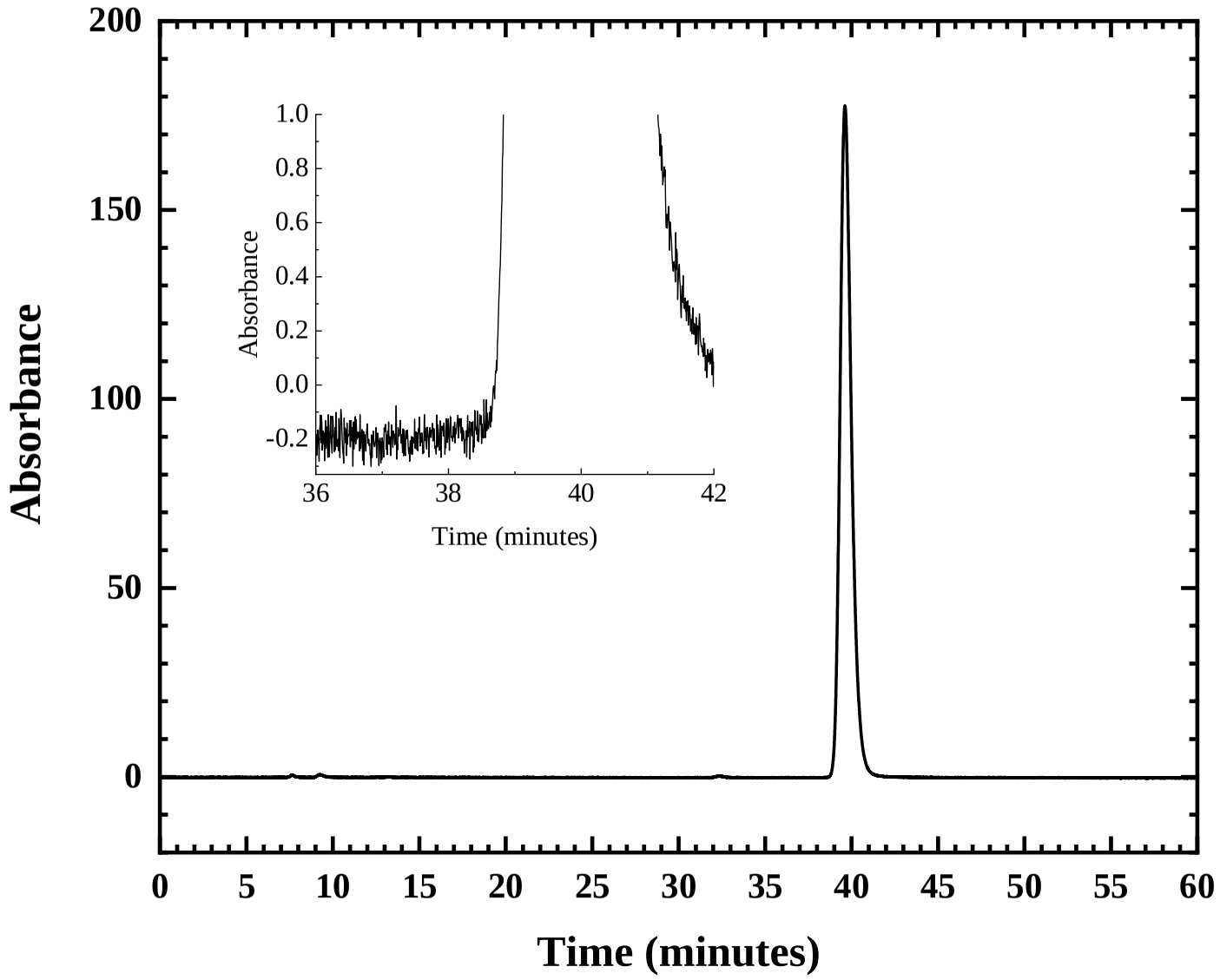

Figure A17: Re-analysis of an extracted fraction at a retention time of 40 minutes using a 100 µL injection, a mobile phase of toluene/n-hexane (70:30), and a flow rate of 2.000 mL/min.

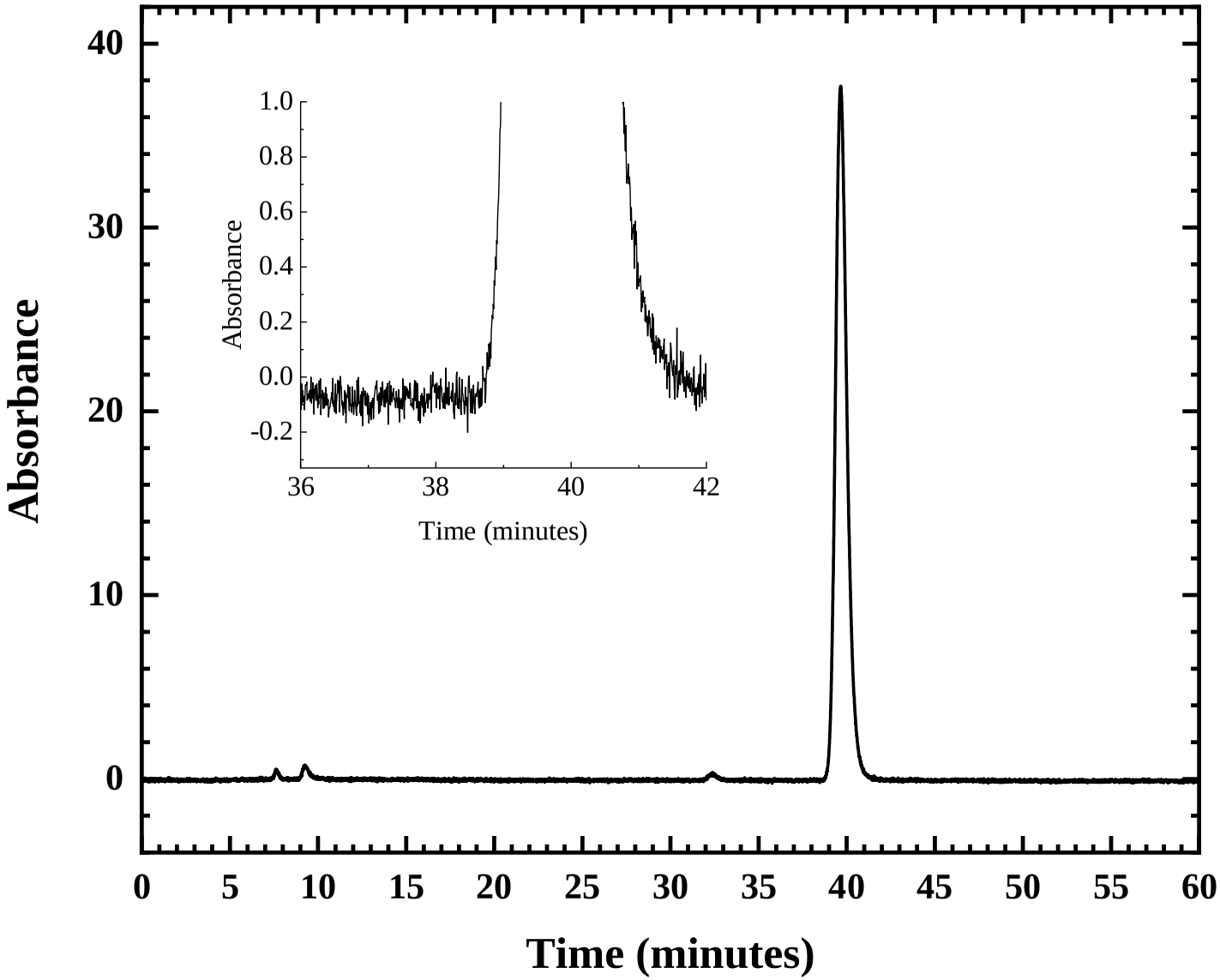

Figure A18: Re-analysis of an extracted fraction at a retention time of 41 minutes using a 100 µL injection, a mobile phase of toluene/n-hexane (70:30), and a flow rate of 2.000 mL/min.

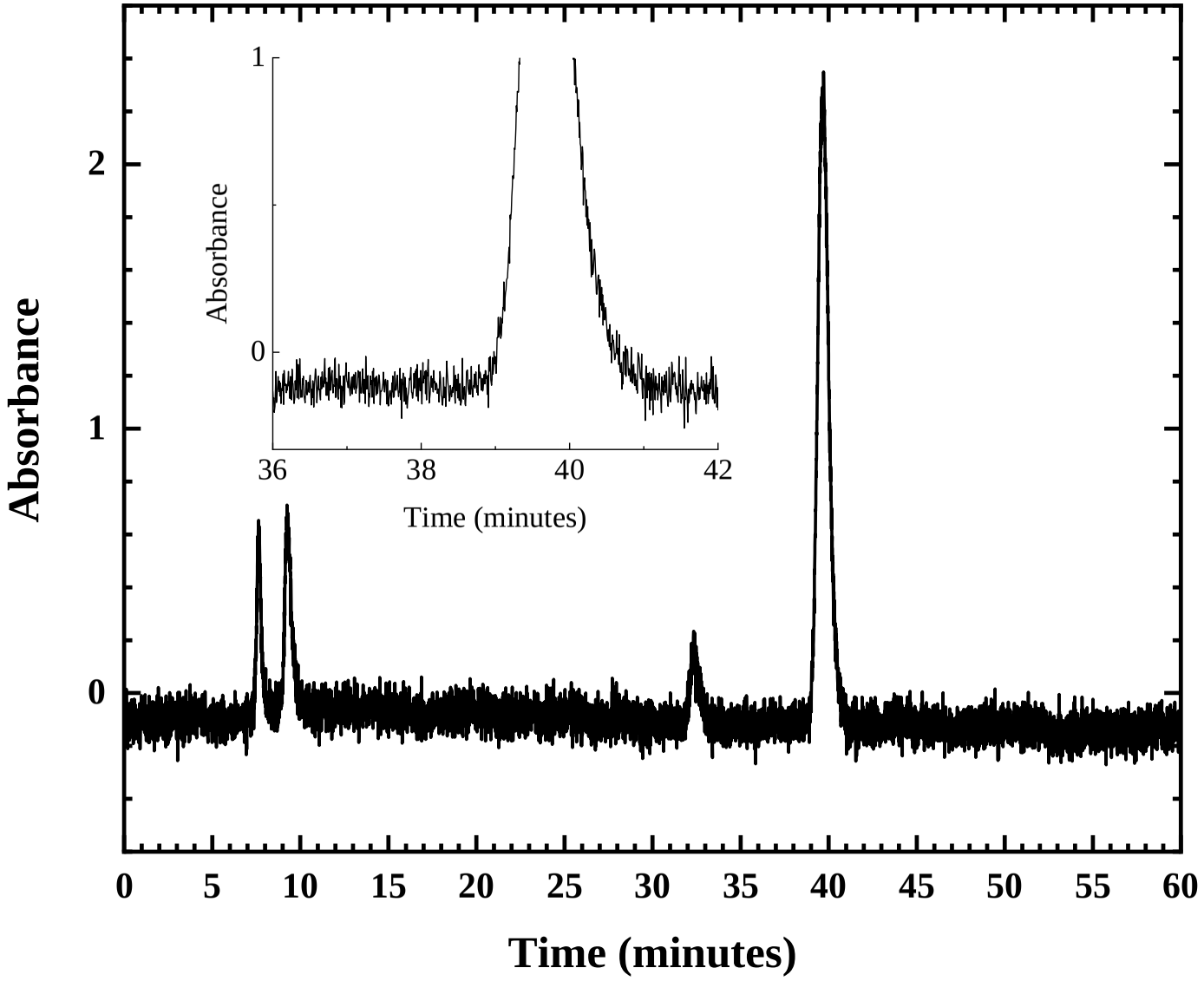

Figure A19: Re-analysis of an extracted fraction at a retention time of 42 minutes using a 100 µL injection, a mobile phase of toluene/n-hexane (70:30), and a flow rate of 2.000 mL/min.